Copper nanocatalysts applied in coupling reactions: a mechanistic insight

Marc Camats, Daniel Pla, Montserrat Gómez

REVIEW ARTICLE

Copper nanocatalysts applied in coupling reactions: a mechanistic insight

Received 00th January 20xx,
Accepted 00th January 20xx

DOI: 10.1039/x0xx00000x

Marc Camats,[a] Daniel Pla*[a] and Montserrat Gómez*[a]

Copper-based nanocatalysts have seen a great interest in synthetic applications since the early 20th century, as evidenced by the exponential number of contributions reported (since 2000, more than 48,000 works published out of about 81,300 since 1900; results of SciFinder using "copper nanocatalysts in organic synthesis" as keywords). These huge efforts are mainly based on two key aspects: i) copper is an earth abundant metal with low toxicity, leading to inexpensive and eco-friendly catalytic materials; and ii) copper can stabilize different oxidation states (0 to +3) for molecular and nanoparticle-based systems, which promotes different types of metal-reagent interactions. This chemical versatility allows different pathways, involving radical or ionic copper-based intermediates. Thus, copper-based nanoparticles have become convenient catalysts, in particular for couplings (both homo and hetero-couplings), transformations present in a remarkable number of processes affording organic compounds, which find interest in different fields (medicinal chemistry, natural products, drugs, materials…). Clearly, this richness in reactivity makes understanding the mechanisms more complex. The present review focuses on the analysis of reported contributions using monometallic copper-based nanoparticles as catalytic precursors applied in coupling reactions, paying attention to those shedding light on the reaction mechanism.

1. Introduction

Coupling reactions are known since the middle of the 19th century when Charles A. Wurtz described in 1855 the homo-coupling of alkyl halides using sodium as reducing agent.[1] Later, in 1869, Carl A. Glaser reported the coupling of terminal alkynes using stoichiometric amounts of copper[2] and in 1901, Fritz Ullmann published the coupling of aryl halides.[3] Cross-couplings promoted by copper were first described by F. Ullmann[4] and Irma Golberg[5] in 1905 and 1906, respectively. Despite these relevant contributions, copper was not largely applied in organic synthesis until the 1960's, probably due to experimental limitations associated with pioneer works, such as high temperature, high metal loading, reaction hazards and relatively low tolerance to functional groups.[6] Advances in innovative ligands and a better understanding of reaction mechanisms facilitated the design of copper-based catalysts overcoming the initial issues. On top of that, copper is a relatively abundant metal (70 ppm of the earth's crust *versus* 0.015 ppm for Pd) with low toxicity, resulting in less expensive and more sustainable catalysts than those involving heavier transition metals. Currently, copper represents a competitive alternative to palladium, from an environmental and economical point of view. This trend is clearly evidenced by the exponential reported contributions since 2000 (Fig. 1).

From a mechanistic point of view, the interest of copper in organic synthesis is mainly motivated by two key aspects. First, copper is capable of stabilizing different oxidation states (from 0 to +3) permitting both one- and two-electron transfer (*i.e.* radical and polar) pathways. Second, copper can easily bind to heteroatoms and favour both σ- and π-interactions with unsaturated functional groups. Furthermore, copper exhibits the ability to form coordination and organometallic complexes, and also well-defined nanoparticles, tuning their structures and compositions due to the copper oxidation state and the nature of ancillary ligands (or stabilisers for metal-based nanoparticles). In terms of applications view, the use of both heterogenised molecular-based catalytic systems and copper-based (un)supported nanoparticles allow a straight-forward catalyst recycling, working under batch or flow conditions.

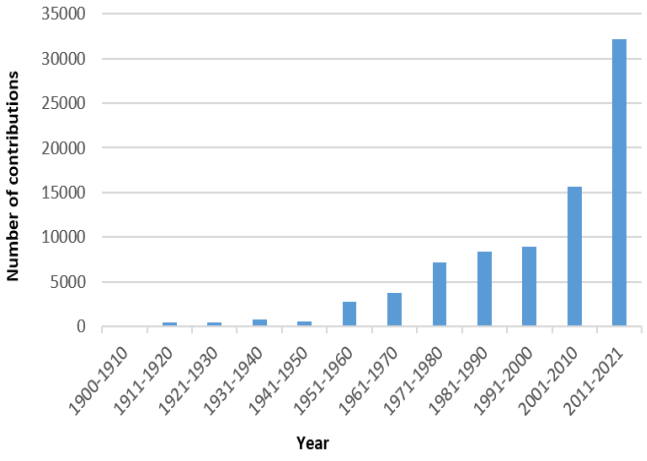

Fig. 1 Publications in the period 1905-August 2021 using "copper nanocatalysts in organic synthesis" as search topic (data collected from SciFinder database).

[a] *Laboratoire Hétérochimie Fondamentale et Appliquée, UMR CNRS 5069, Université Toulouse 3 – Paul Sabatier, 118 route de Narbonne, 31062 Toulouse cedex 9, France. Email: pla@lhfa.fr; gomez@chimie.ups-tlse.fr*

Nanocatalysis using metal nanoparticles as catalytic precursors represents a fast developing area with broad applications in chemical synthesis.[7] Small-sized metal nanoparticles ranging from 1–10 nm in diameter exhibit distinct catalytic activities, often better than the parent molecular complexes or heterogeneous catalysts. This catalytic behaviour is mainly due to the extended surface areas of nanomaterials, which compared to bulk materials, exhibits a higher concentration of defects at the surface and low-coordinated metal centres providing a high concentration of highly reactive sites. The small size of nanoparticles does provide a particular set of electronic and quantum effects which may unlock catalytic pathways only allowed by the use of nanocatalysis. Metal nanoparticles immobilised both in solution and solid supports, find efficient applications due to their facile recovery without losing their catalytic properties, which makes them environmentally friendly.[8]

Current methods of metal-based nanoparticles encompass catalyst preparation by reduction of Cu(I) and Cu(II) salts and organometallic complexes (such as CuI, mesitylcopper(I), $Cu(OAc)_2$ or $Cu(NO_3)_2$) in the presence of solid supports or liquid phases.[9] Despite copper species shall be completely reduced to zero-valent copper nanoparticles, electron deficient $Cu^{\delta+}$ sites via the loss of electrons at the Fermi level or even residual cationic copper species (showing different oxidation states) may be of paramount importance in enabling reactivity and selectivity trends. This nanoparticle feature induces a certain flexibility at the metal centres, in terms of charge stabilisation, especially important throughout electron transfer steps, from both thermodynamic and kinetic point of view.

The soft Lewis acidity of such cationic species on small Cu nanoparticles may be responsible for the catalytic activity. Despite the elucidation of the catalytic active species is challenging because the variety of copper oxidation states (*i.e.* 0, +1, +2 and +3) and many organic reactions can be catalysed by Cu(I), Cu(II) or Cu(III) complexes and by copper-based nanoparticles (Cu(0), Cu_xO_y, Cu_xS_y…), the rational design of catalytic systems is key towards reaction optimization and catalytic performance enhancement (*e.g.* conversion and selectivity) of nanocatalysts, required to move forward more sustainable applications.[10]

From a mechanistic point of view, nanoparticles morphology (*i.e.* size, shape and structure) is crucial for understanding the catalytic reactivity, in particular the recognition and quantification of the active sites.[11] Regarding size, small nanoparticles (1-5 nm) exhibits a suitable compromise between active surface and structure stability. However, MNPs morphology often varies during the catalytic reaction, due to the formation of diverse intermediates that can trigger morphological changes (Fig. 2).[12] For these purposes, modelling studies represent an essential tool which enables correlating calculations with experimental data. Recently, Maestri, Mpourmpakis and co-workers have modelled the catalytic reactivity and morphology of MNPs under reaction conditions (in particular for RhNPs applied to the dissociation of CO), by Boltzmann statistics and DFT calculations, for the most stable nanoparticles and the ensemble of nanoparticles. The correlation between reactivity in terms of different active sites was in good agreement with experimental data.[13] However, the multi-component reactions make these methods difficult, due to the multiple interactions to be considered. Zheng and co-workers have carried out a meaningful work on coordination of organic molecules to defined metallic clusters with the aim of using them as models for surface coordination chemistry of MNPs.[14]

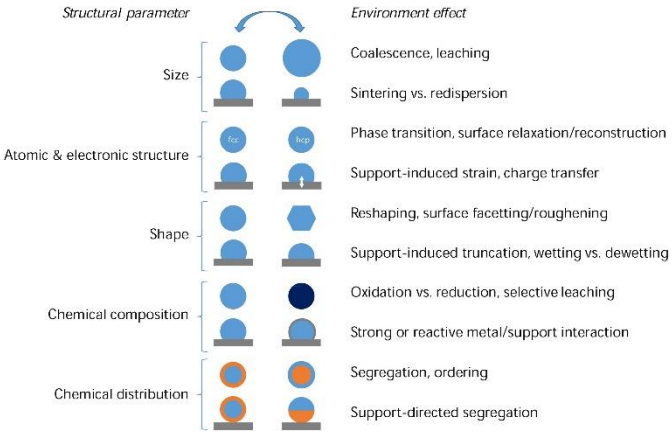

Fig. 2. Some examples of MNP morphology changes produced under catalytic conditions. Adapted from [12] with permission of Elsevier and Copyright Clearance Center (license number: 5160190892244) 2021.

On the other hand, the incessant progresses on characterization techniques, in particular those based on real-time approaches, lead to a better understanding of the catalytic transformations. In this review, advances in mono-metallic copper-based nanocatalysts for organic synthesis purposes are discussed, highlighting those contributions with mechanistic approaches.

2. Homocoupling reactions

2.1. C(sp)-C(sp) homocoupling reactions

Since the first copper-mediated acetylenic homo-coupling reaction reported by Glaser back in 1869, where copper(I) phenylacetylide underwent dimerization under aerobic conditions to deliver diphenyldiacetylene,[2,15] followed by a catalytic version (Hay modification) using nitrogen donor ligands such as *N*,*N*,*N*′,*N*′-tetramethylethylenediamine (TMEDA) which facilitated the reaction under homogeneous and aerobic conditions,[16] progress has been made on the elucidation of activation mechanisms of terminal alkynes via σ- and π-bond coordination modes with low-valent Cu catalysts, namely Cu(0) or Cu_2O, but the higher complexity of nanostructured systems in comparison to classical molecular or heterogeneous systems demands cutting-edge characterization methods to speed innovation in this field.

Copper nanocatalysts, mainly immobilised systems, have provided a greener route towards the production of 1,3-diynes, allowing metal recovery and catalyst reusability and at the same time providing safer procedures. Often being able to replace the use of pure oxygen by air and avoiding refluxes of flammable solvents. Thus, this section summarizes the recent advances in Cu(0) and Cu_2O NPs catalysed C(sp) homocoupling reactions to

yield symmetrical 1,3-diynes products with special emphasis on the catalyst morphology, oxidation state and support. Although the specific role of small nanoparticles (1-10 nm) in the reaction mechanisms is challenging to ascertain, such nanoparticles have been demonstrated to exhibit unique catalytic properties. Radivoy and co-workers have reported the use of very reactive and monodisperse (3.0 ± 1.5 nm), spherical low valent copper nanoparticles in-situ generated from anhydrous $CuCl_2$ and lithium sand (in equimolar amounts).[17] Despite the lack of stabilizing agents triggered particles agglomeration (up to 15-30 nm diameter sizes after THF reflux for 6 h), this catalytic system permitted the homocoupling of traditionally sluggish alkylacetylenes under N_2 (Scheme 1). The authors have validated the role of the base in enhancing reaction rates and propose the formation of alkynyl-Cu complexes, but claim for further studies to ascertain the differential reaction mechanism of Cu(0) NPs versus the classical one via Cu(I)-acetylide intermediates. Indeed, the role of lithium alone via the formation of more complex bimetallic systems could not be excluded at this time.

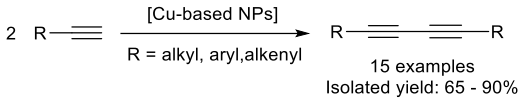

Scheme 1 Homocoupling of alkynes.[17]

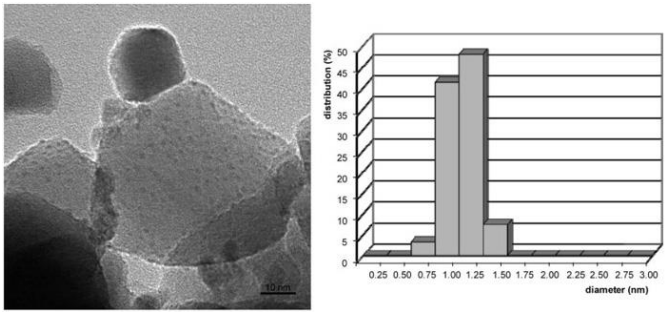

Fig. 3 TEM micrograph of Cu_2O NPs@TiO_2 catalyst and size distribution analysis for 125 nanoparticles randomly selected. Adapted from [19] with permission of John Wiley and Sons and Copyright Clearance Center (license number: 5143150408233) 2011.

These authors have adapted their methodology to support Cu-based NPs (ca. 3 nm) on silica-coated maghemite supports of nanometric size ranging from 5-30 nm in particle size.[18] The as-prepared composite catalyst showed easy catalyst recovery and negligible leaching of metal species. A similar strategy has been used by Alonso, Yus and co-workers for the immobilization of Cu_2O nanoparticles onto a high surface area TiO_2 support (featuring 60% anatase and 40% rutile polymorphs).[19] Despite doubling the amount of reducing agent (lithium powder) to reduce $CuCl_2$ in comparison to the precedent report, the copper catalyst was mainly in the form of ultrafine Cu_2O NPs of 1.0 ± 0.4 nm average diameter size (Fig. 3), as denoted by the analysis of the Auger spectrum and the absence of satellite peaks of Cu(II) species in the XPS spectrum. Mechanistic studies on the nature of the catalytic process pointed to a surface catalysed reaction as a slight conversion increase was observed after reuse of the catalyst upon removal of the supernatant solution with a negligible copper leaching (45 ppb of copper detected by ICP-MS analyses). As in the parent non-supported catalyst, catalysis takes place under inert atmosphere, overriding the need of oxygen and no alkynyl radicals could be detected.

In addition, alternative bottom-up chemical methods have been mostly used for the preparation of low-valent Cu-based NPs systems in combination with either solid supports such as SiO_2 (Scheme 2),[20] covalent organic frameworks[21] or ionic liquids.[22] Thus, Luque and co-workers have described the preparation of highly active Cu_2O-CuO NPs on self-assembled silica nanotubes exhibiting high surface areas (90–500 m^2g^{-1}).[20] The synthesis of the catalyst composite featuring Cu_2O NPs (34 ± 4 nm average size) was achieved in one pot by reaction of $CuCl_2$, $Si(OEt)_4$ and dodecylamine at temperatures ranging from 80 to 110 °C under microwave irradiation. High reaction conversions (>90%) and good homocoupling selectivity (75%) is obtained. However, the presence of mixed oxidation states in the catalyst composition (up 40% of Cu(II) species as determined by XPS analysis) may merit further investigation in terms of reaction selectivity improvement.

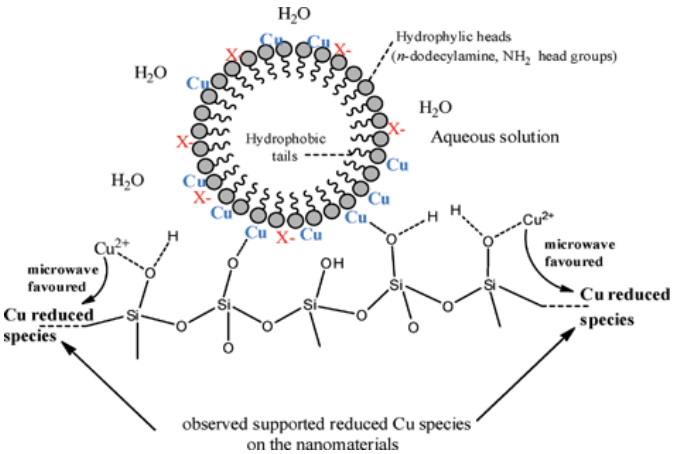

Scheme 2. Proposed mechanism of tubular nanostructure formation via the reduction of Cu(II) species by silanol groups promoted under microwave irradiation. Reprinted from [20] with permission from the Royal Society of Chemistry.

Bottom-up approaches have also been used for the preparation of low-valent Cu-based NPs systems in combination with polymeric supports. Thus, as reported by Zuraev and co-workers, Cu(0) NPs supported on polymer matrixes exhibit higher stability of the particles and protection against oxidation despite their inherent sensitivity to oxygen and water.[23] In addition, the nitrogenated matrix prepared by thermolysis of a copper(II) poly-5-vinyltetrazolate polymer enhanced mass transfer of substrate during the reaction resulting in high catalytic activities. PXRD analysis of the catalytic material revealed only the presence of Cu(0) nanocrystalline phases of 30 nm average diameter size, however the authors do not report XPS data that could take into account amorphous copper phases. Moreover, the formation of well-dispersed Cu nanoparticles of 6.5 ± 1.5 nm average diameter size supported in a polyaniline matrix has been reported by Ul Islam and co-workers.[24] They used an *in situ* polymerisation approach using $CuSO_4$ as the oxidizing agent encompassing the formation of a

Cu(I)-composite material which was then subjected to $NaBH_4$ reduction to form Cu(0) NPs@polyaniline. The authors confirmed that the homocoupling of terminal alkynes was facilitated under aerobic conditions, arguably due to the fact that the base and oxygen present in air helps the formation of Cu(I)–acetylide intermediate species capable to deliver the homocoupling product by reductive elimination. Analogously, Yao and co-workers described the synthesis of low-valent Cu NPs by $NaBH_4$ reduction of $Cu(OAc)_2$ in EtOH at 40 °C for 20 h in the presence of ordered mesoporous carbon nitride materials (OMCN, prepared by polymerization of 2,4,6-trichlorotriazine with benzidine in the presence of SBA-15 as template).[25] The PXRD pattern of the prepared Cu NPs@OMNC showed the characteristic two diffraction peaks at 43.6° and 50.5° corresponding to the (111) and (200) lattice planes of metallic Cu fcc structure, but the appearance of Cu_2O (111) was also observed. TEM analysis of the Cu-based NPs@OMCN showed the copper nanoparticles successfully supported on the hexagonal mesopores of 4.7 nm pore size. Balova and co-workers have recently reported the preparation of C(sp) homocoupling-selective copper-based nanocatalysts by *ex situ* laser-induced methods from copper precursors such as $CuCl_2$ and $Cu(OAc)_2$.[26] This methodology adds up to the classical bottom-up approaches.

Differential activation pathways under molecular regimes have been reported for Cu(II)-mediated oxidative homocoupling of terminal alkynes in the presence of pyridine as ligand,[27] as first reported by Eglinton in the late 1950s.[28] In particular, two key mechanistic steps have been described for this coupling type under homogeneous conditions, namely a π-bond coordination of the triple bond to electrophilic Cu(II) species that weakens the terminal C–H bond, thus facilitating its deprotonation by a base, as well as a final reductive elimination step from a dinuclear copper(II) acetylide species (Scheme 3).[27,29]

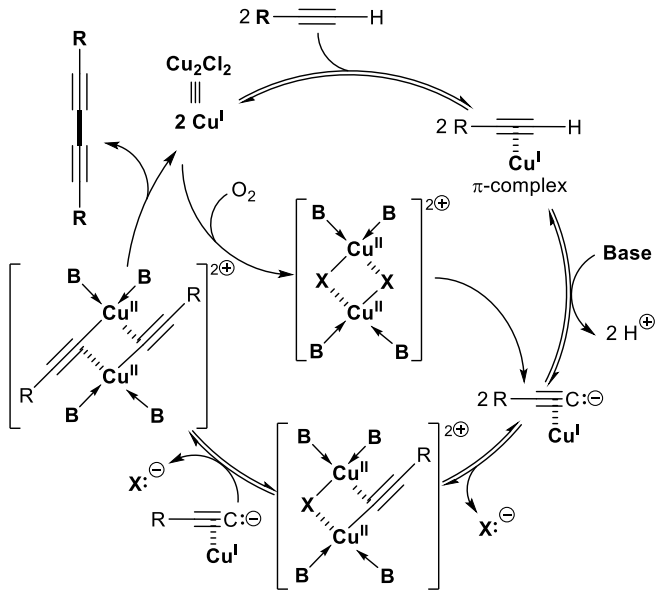

Scheme 3. Bohlmann mechanism for the Glaser homocoupling of acetylenes (B = N ligand).[29] *Note: for each proposed intermediate, the oxidation state on the copper sites is indicated on each copper ion (roman numbers); the total charge of intermediates is indicated together with the square brackets.*

Hitherto, only copper oxide based nanocatalytic systems have been described featuring Cu(II) species for applications in homocoupling reactions (Fig. 4).[30] As an example, Kaur and co-workers have described the synthesis of uniformly distributed CuO NPs (6 ± 3 nm size) on an Amberlite XAD-4 polystyrene resin featuring nitro group functionalization.[30a] The nitro groups played an important role in the coordination of copper(II) cations from $Cu(OAc)_2$ precursor on the resin, which was then subjected to $NaBH_4$ treatment. XPS and XRD analyses of the as-prepared material revealed the presence of core-shell structure, featuring a Cu(0) core covered with an oxide layer on the surface.

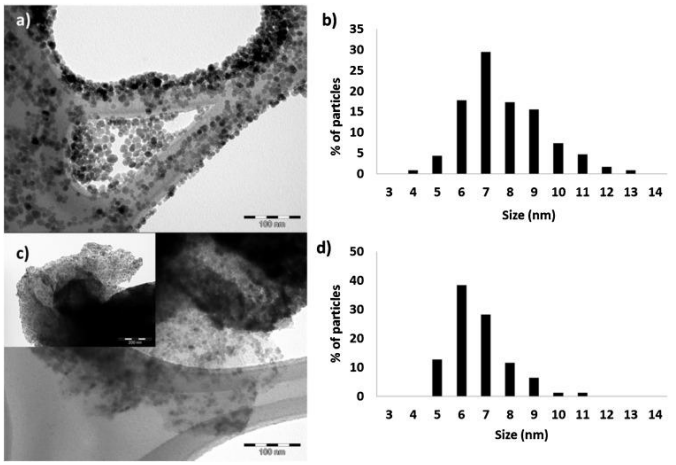

Fig. 4 TEM micrograph of CuO_x NPs@Fe_3O_4 (a) and its particle size distribution graphic (b); TEM micrograph of CuO_x-Fe_3O_4 NPs@graphene (c) and its particle size distribution graphic (d). Reproduced from [30d] with permission of Elsevier and Copyright Clearance Center (license number: 5160240128897) 2017.

Jones and co-workers assessed the heterogeneity of CuO NPs (17-72 nm in size) supported on both γ-Al_2O_3 and TiO_2 precatalysts in ethynylbenzene oxidative homocoupling in the presence of piperidine as a base,[30b] revealing that the formation of soluble molecular copper-piperidine complexes at elevated temperature was needed to form the catalytically active species, so the reaction could then proceed even at room temperature with good conversions towards the homocoupling product. Besides, Serp, Raspolli-Galletti and co-workers[30d] have successfully prepared magnetic copper oxide based nanoparticles on nanosized magnetite supports. The catalyst composite (featuring 9-13 nm particles of both CuO_x and Fe_3O_4) exhibit high selectivity towards phenylacetylene oxidative homocoupling in the absence of an external base, and thus probably precluding both metal leaching and formation of molecular copper-base complexes thanks to synergistic effects between CuO_x and magnetite support. XPS data revealed the presence of mostly Cu(II) on the catalysts surface, but the characteristic face centred cubic Cu_2O peaks were also detected by PXRD. In addition, it has been shown by Rossi, Suib and co-workers for analogous CuO@MnO_x catalytic systems that the support (manganese oxide) assists the re-oxidation of low-valent Cu species formed during catalysis in air.[30c] To illustrate the oxidative coupling of alkynes on the CuO@MnO_x surface, the authors propose that the π-$[Cu^{II}(HC{\equiv}CH)(H_2O)_4]^{2+}$

interaction via a three-electron stabilizing interaction (Fig. 5a, analogous to a molecular Glaser-Hay mechanism) is more stable than the corresponding Cu(I) one. In addition, the authors propose a model system involving a η^2:η^2-peroxo motif (Fig. 5b), but further mechanistic studies are required to assess the higher activities and maximize the synergistic effects operating in MnO_x since Mn atoms from the support may not only form stable $Mn^{III}O_2(H_2O)_n$ in the presence of air, which are capable of proton abstraction from bonded acetylene units in close proximity, but also these Mn sites neighbouring active Cu atoms may interact with the approaching acetylide anionic fragments and accommodate the two discarded electrons arising from the oxidation of acetylide anions via Mn available 3d orbital, as discussed by the authors.[30c]

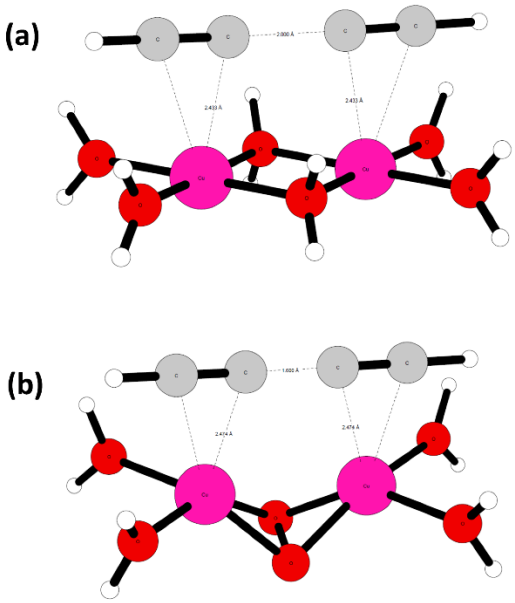

Fig. 5 Model systems of CuO@MnOx surface in the oxidative coupling of alkynes: (a) Cu atoms in adjacent positions to each other; (b) O_2 as bridging ligand between Cu sites. Adapted with permission from [30c]. Copyright 2016 American Chemical Society.

2.2. C(sp²)–C(sp²) homocoupling

Cu-catalysed C(sp²)–C(sp²) homocoupling reactions pioneered by Ullmann in 1901 for the synthesis of symmetrical bis-aryls,[3] represent a distinctive activation mode that has been widely applied in synthesis. Despite the broad substrate scope for this transformation, comprising aryl halides, arylboronic acid derivatives, or other organometallic reagents, and even unactivated arenes, correlation studies taking into account the catalyst nature (phase, oxidation state, synergistic effects…) and mechanistic insights are key to the development of novel catalyst systems with enhanced properties in terms of activity, selectivity and recyclability. Although this reactivity has been known for a long time and is still, the progress on the development of well-defined catalysts at the nanometric scale urges fundamental studies to elucidate the reaction mechanisms governing these type of transformations. Thus, this section summarizes the recent advances in Cu-based NPs catalysed C(sp²) homocoupling reactions to yield symmetrical bisaryls products with special emphasis on the catalyst morphology (particle size, shape, homogeneity…), oxidation state and support (Scheme 4).

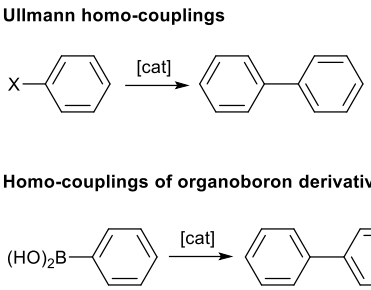

Scheme 4 C-C homo-coupling reactions catalysed by Cu-based NPs covered in this review (reaction conditions and concomitant products have been omitted).

The catalyst system developed by Chu, Sun and co-workers by reduction of $CuSO_4$ with ascorbic acid in the presence of graphene oxide in *N*-methylpyrrolidone as solvent at 90 °C for 2 h featured Cu(0) NPs (ca. 8 nm in size, Scheme 5).[31] Despite the synthesis conditions triggered a partial reduction of the graphene oxide support, the as-prepared catalyst composite resulted highly active towards the homocoupling of aryl halides. Despite the high efficiency obtained for the conversion of both aryl iodides and bromides bearing electrodonating and electrowithdrawing groups in DMF, DMSO or a mixture of 1-butyl-3-methylpyridinium bis(trifluormethylsulfonyl)imide and water as solvent under microwave irradiation (70-90 W) for 30 min, aryl chlorides were also reactive substrates albeit in moderate yields. This catalyst composite showed high activity towards the homocoupling reaction of boronic acid substrates, but further studies towards the elucidation of the differential elementary steps (oxidative addition, transmetallation…) involved in the activation of both types of substrates are needed. In an analogy with homogeneous systems, Ph-$B(OH)_2$ bond activation via transmetallation is the key step in the oxidative homocoupling of organoboronic acid derivatives.[32] Cu(0) nanocatalysts generated by reduction of $CuCl_2$ precursor with Li powder have also been proposed by Radivoy and co-workers as active catalysts for the homocoupling of aryl, heteroaryl and alkenyl Grignard reagents (Fig. 6).[33] As discussed in the previous section for analogous catalysts prepared by this methodology, further studies to assess the role of lithium cooperative effects and the mechanism of transmetallation are needed.

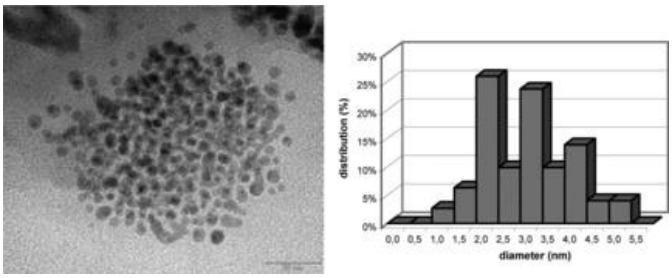

Fig. 6. TEM image of Cu NPs their and size-distribution graphic (out of 200 particles). Reprinted from [33] with permission from Taylor & Francis Ltd (www.tandfonline.com).

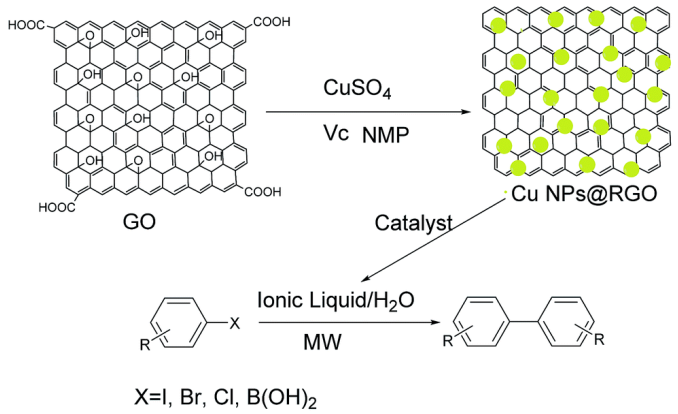

Scheme 5. Synthesis of Cu NPs on reduced graphene oxide and their use as catalyst in homo-coupling reactions. Reprinted from [31] with permission from the Royal Society of Chemistry.

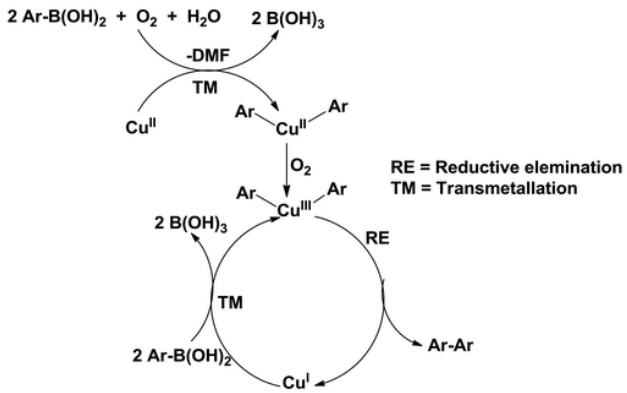

Scheme 6 Proposed mechanism for the oxidative homocoupling of arylboronic acids based on a monometallic active centre. Adapted from [38b] with permission from the Royal Society of Chemistry.

Core-shell Cu-Cu_2O based nanocatalytic systems featuring a Cu(0) metal core (with crystallite size of 8-12 nm in diameter) encapsulated by a layer of amorphous copper oxide (20-45 nm overall diameter size) have been prepared by Klabunde and co-workers via the solvated metal atom dispersion (SMAD) method.[34] The authors could establish a positive correlation between the chemical reactivity towards Ullmann reaction and the surface area of the as-prepared catalytic systems.

Parvulescu, Garcia and co-workers have recently prepared graphene-film supported Cu_2O nanoplatelets (8 nm in size) by one-step pyrolysis of $Cu(NO_3)_2$ embedded in chitosan at 900 °C under inert atmosphere that were active towards the homocoupling of iodobenzene in the absence of base.[35] Studies on the catalytic regimes of Cu_2O-nanoparticle-catalysed C–C couplings carried out by Andiappan and co-workers[36] indicate that Cu_2O systems can catalyze homocoupling reactions precluding the need of ligands or base via surface reactivity, enabling their implementation in flow applications.

The heterogeneous nature of analogous CuO nano-rod shaped catalysts has been reported by Veer and co-workers in the oxidative homocoupling of arylboronic acids via hot filtration tests and the absence of copper leaching.[37] Thus, upon removal of the nanocatalyst, no further reaction conversion was observed in the filtrates (monitoring during 6 h). Despite the lack of appreciable changes in the CuO PXRD pattern of the fresh and the reused catalyst after the 5th run, the authors proposed a mechanism based on a monometallic active center encompassing a double transmetallation on a Cu(II) site, followed by air oxidation to generate the corresponding bis-aryl Cu(III) reactive intermediate that undergoes reductive elimination, generating biphenyl as a product and reduced Cu(I) species (Scheme 6). While this is in agreement with precedent mechanisms described for the oxidative homocoupling of arylboronic acids under homogeneous regimes,[38] the possibility of cooperative effects among neighbouring copper atoms cannot be ruled out.[37]

3. C-C cross-couplings

Since 1960's, C-C cross-coupling reactions applied in organic synthesis have been generally associated to palladium-catalysed processes, internationally recognized with the Nobel Prize in Chemistry 2010 awarded to R. F. Heck, E.-I. Negishi and A. Suzuki.[39] Although the copper ability to form C-C and C-N bonds is known since 1905 and 1906 by the pioneer works independently published by F. Ullmann[4] and I. Goldberg[5] respectively, Cu-catalysed cross-couplings have been extensively developed from the end of the 20th century (more than 105,000 reports have been found in SciFinder database in the period 2000-2021, answering to the topic "copper-catalysed cross-couplings" *versus* 99,883 reports for a similar search concerning palladium).[6c,40] In this section, C-C cross-couplings are described. C-heteroatom bond formation processes are presented in section 4 (see below).

3.1. Alkyne cross-coupling

Unsymmetrical 1,3-diynes are present in many intermediates involved in organic synthesis and also appear as structural motifs in functional materials and natural products.[41] The most important challenge in the heterocoupling of two different terminal alkynes catalysed by homogeneous or heterogeneous systems, is the chemoselectivity, often controlled by using a large excess of the less reactive alkyne (*i.e.* more electron rich reagent).[42] Thus, this challenge often turns the catalyst design into a game of kinetics and statistics.

Although high selectivity towards unsymmetrical diynes is not trivial to be achieved, some Cu-based nanocatalysts have been recently reported, obtaining high isolated yields. [21, 43]

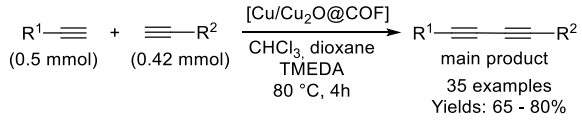

Fig. 7 Substrate scope for the synthesis of unsymmetrical diynes catalysed by Cu/Cu_2O nanoparticles immobilised on phenol-pyridiyl covalent organic frameworks (COF).[21]

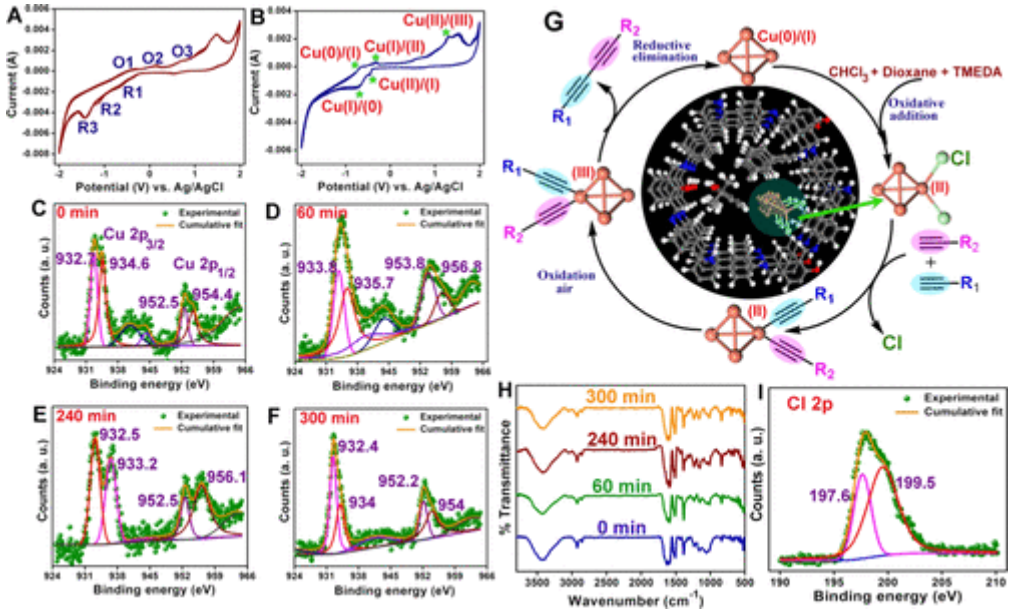

Fig. 8 Characterisation of Cu-based NPs supported on COF (Cu@COF): Cyclic voltammetry of Cu@COF showing the reversible formation of Cu(0)-Cu(I)-Cu(II)-Cu(0) species (**A** and **B**: O means oxidation wave; R, reduction wave); XPS spectra at the Cu 2p binding energy region for Cu@COF (t = 0 min) and at different stages of the reaction (**C**-**F**); IR spectra of the catalyst at different reaction times showing no change of COF (**H**); XPS spectrum at Cl 2p binding energy region of an isolated sample of Cu@COF during the catalytic reaction, proving the presence of Cu-Cl species (**I**). Reprinted with permission from [21]. Copyright 2019 American Chemical Society.

From a mechanistic point of view, it is important to highlight the contribution of Vinod, Vaidhyanathan and co-workers, which prepared Cu/Cu_2O NPs (mean size Cu-based NPs: 2-3 nm determined by HRTEM analyses) confined on covalent organic frameworks (COF), exhibiting H-protonable pyridyl-lined and H-bonding hydroxyl pores.[21] This catalytic material was successfully applied in heterocouplings of terminal alkynes using a nearly equimolar ratio of both alkynes: 0.5/0.42 (Fig. 7). This hybrid catalyst was able to stabilize Cu-Cl based clusters formed from chloroform (used as solvent), which were responsible of the observed reactivity.

A thorough characterization study of the catalytic material (cyclic voltammetry, XPS, IR) at different reaction times evidenced the presence of high-valent metal species, observing a reversible oxidation of Cu(0)/Cu_2O into Cu(II) and Cu(III)), where the COF structure tunes the redox activity (Fig. 8). DFT calculations suggested that the functionalized pores of the support favour the interaction of hetero-substrates (two different alkynes) with the catalyst rather than with homo-substrates (two identical alkynes), in agreement with the experimental results.

3.2. Sonogashira-type couplings

C-C cross-couplings involving terminal alkynes and aryl or vinyl halides (or triflates) mainly catalysed by palladium and copper species also including palladium- and copper-free versions, represent a valuable and widely used tool for the synthesis of biologically active molecules, natural products, molecular electronics and polymers, through C(sp^2)-C(sp) bond formation reactions.[44]

For Cu-catalysed Sonogashira reactions, many research works have been reported in the literature, most of them concerning Cu(I) or Cu(II) salts and coordination complexes as catalytic precursors,[45] designing catalysts and reaction conditions in order to avoid the competing Glaser-Hay homocoupling and to allow working under safe conditions (some Cu(I)-acetylene organometallic complexes can be explosive). From a mechanistic point of view, a homogeneous pathway is generally accepted involving Cu(I) and Cu(II) intermediate species[46] or concerted activation of C-halide bond and C-C bond formation.[47]

The use of copper-based nanoparticles as catalytic precursors has been less applied. Rothenberg and co-workers reported for the first time Sonogashira-type couplings with different aryl iodides and bromides catalysed by copper clusters, proposing a mechanism where the positive charge generated on copper in the oxidative addition step can be shared among the metal atoms of the cluster, in contrast to happen using homogenous systems, and without formation of high-valent copper species. Thus, this elementary transformation is kinetically favoured, which is often the rate determining step (Fig. 9).[48] It is important to highlight that reagents/metal surface interactions were not deeply studied; it is suggested that phenylacetylene coordinates to the metal cluster leading to an alkenyl-Cu intermediate (probably by a σ bond between Cu and the alkenyl group), and the corresponding aryl halide probably coordinates to copper by π interaction involving several metal centres.

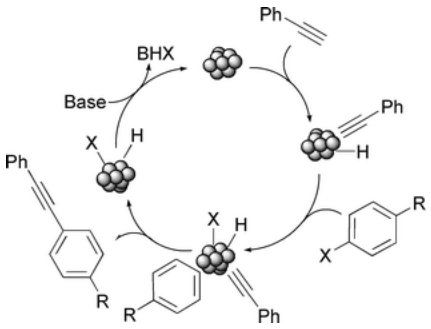

Fig. 9 Proposed cycle for Cu-catalysed Sonogashira coupling. Reproduced from [48] with permission from the Royal Society of Chemistry.

Later on, Cu-based nanoparticles were efficiently applied in this type of couplings, both unsupported[36, 49] and immobilised on inorganic solids such as silica[50] and graphene.[51]

Andiappan and co-workers were interested in proving the nature of the catalytically active species, *i.e.* molecular- *versus* surface-like reactivity.[36] In other words, in proving the lack of copper atoms leaching from the metallic surface. Cu_2O nanoparticles were prepared by microemulsion methodology and characterized by TEM (mean size: 34 nm) and PXRD (only presence of Cu_2O crystalline cubic phase). The authors proved (by different techniques applied to the catalytic reactions: UV-vis extinction spectroscopy, ESI-MS, FAAS and TEM) that in the absence of base, molecular species could not be detected, in contrast to the tests carried out in the presence of a base.

3.3. Suzuki-type couplings

Analogously to Sonogashira and Heck reactions, cross-couplings between aryl halides and aryl boronic acids are a useful synthetic methodology, together with Ullmann-type reactions, for the synthesis of bis-aryl compounds, which are present in a wide panel of commercially available products.[52]

As known, these cross-couplings are commonly catalysed by palladium-based systems, both homogeneous and heterogeneous ones. Despite the efficiency of this process (wide scope, high TON, vast applications), in the current trend to replace noble metals by earth-abundant and low-cost metals, innovative catalytic systems are developed. In addition to this reason, copper has been proven to be more efficient than palladium for Suzuki cross-couplings involving highly fluorinated boronate esters.[53] Concerning nanocatalysts, in 2002, Rothenberg and co-workers reported Suzuki couplings catalysed by copper nanoclusters, both monometallic and also polymetallic systems, which exhibited a relative high catalytic activity.[54] More recently, some works have been reported involving preformed Cu(0) and Cu_2O nanoparticles in Suzuki reactions, using low copper loading (less than 0.5 mol%) under relative smooth conditions.[55] The *in situ* formation of Cu_2O nanoparticles has been evidenced by XPS and PXRD analyses, using $CuCl_2$ as catalytic precursor and K_3PO_4 as a base for the synthesis of diarylpyridines.[56] Based on these characterization data and the catalytic behaviour, the authors proposed that the nano-material is responsible of the reactivity observed *via* a Cu(I)-Cu(III) mechanism (Fig. 10).

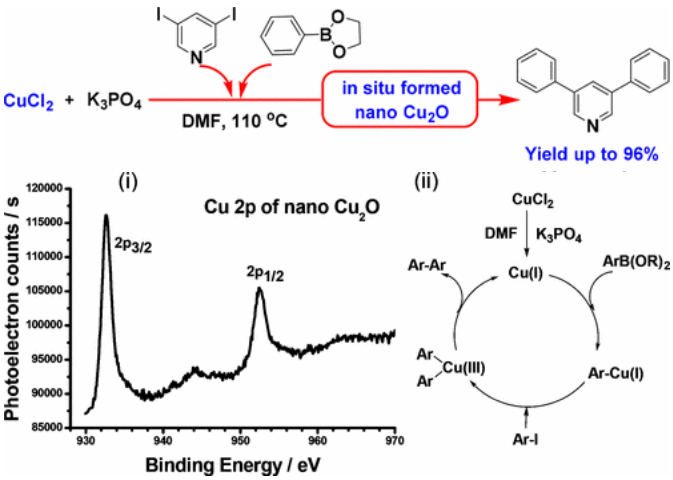

Fig. 10. *Top*: General scheme corresponding to the synthesis of biarylpyridines. *Bottom*: XPS spectrum of Cu_2O nanoparticles at the Cu 2p binding energy region (left); proposed Cu(I)-Cu(III) mechanism for the catalytic reaction. Reprinted with permission from [56]. Copyright 2017 American Chemical Society.

3.4. Cross-dehydrogenative couplings

As very well-known, methodologies for forming C-C bonds represent a decisive role in synthesis design, finding extensive applications in academia and industry.[57] Mostly, these approaches require two functionalized reagents, resulting in the stoichiometric formation of by-products. Since 1990's, a huge work has been developed concerning the activation of C-H bonds, avoiding pre-functionalizations and significantly reducing the generation of wastes.[58] In the frame of these environmentally and economically attractive approaches, the C-H/C-H cross-dehydrogenative coupling (CDC) is a powerful tool for the formation of C-C bonds through the activation of two C-H bonds under oxidative conditions,[59] being copper a versatile catalyst for this type of transformations mainly using metal salts as catalytic precursors.[60] In the last years, the application of well-defined copper-based nanoparticles has been reported,[61] with limited mechanistic studies.[62]

Alonso and co-workers described the CDC of terminal alkynes and tertiary amines catalysed by Cu-based NPs immobilised on different solids, being the most catalytically active and selective system (no formation of diynes) when zeolite was used as support (mean diameter of Cu-based NPs: 1.7 nm).[63] XPS analyses showed that copper was mainly constituted of CuO with the presence of Cu_2O. The authors were interested in studying the mechanism of the reaction. They proved that the reaction occurred under heterogeneous conditions. Thus, the catalyst was separated by filtration from the resulting organic phase at low conversion (*ca*. 5%), evidencing that this solution, under optimized catalytic conditions, did not work (its copper content was negligible: 0.78 ppb by ICP-MS analyses). Control tests with different radical scavengers proved the formation of methyl radicals, coming from the β-cleavage of *t*-butylhydroxyperoxide (TBHP), used as oxidizing agent. XPS analyses of the catalytic material demonstrated that, contrarily to the starting catalytic material, Cu_2O was the main copper phase which was easily re-oxidized with TBHP.

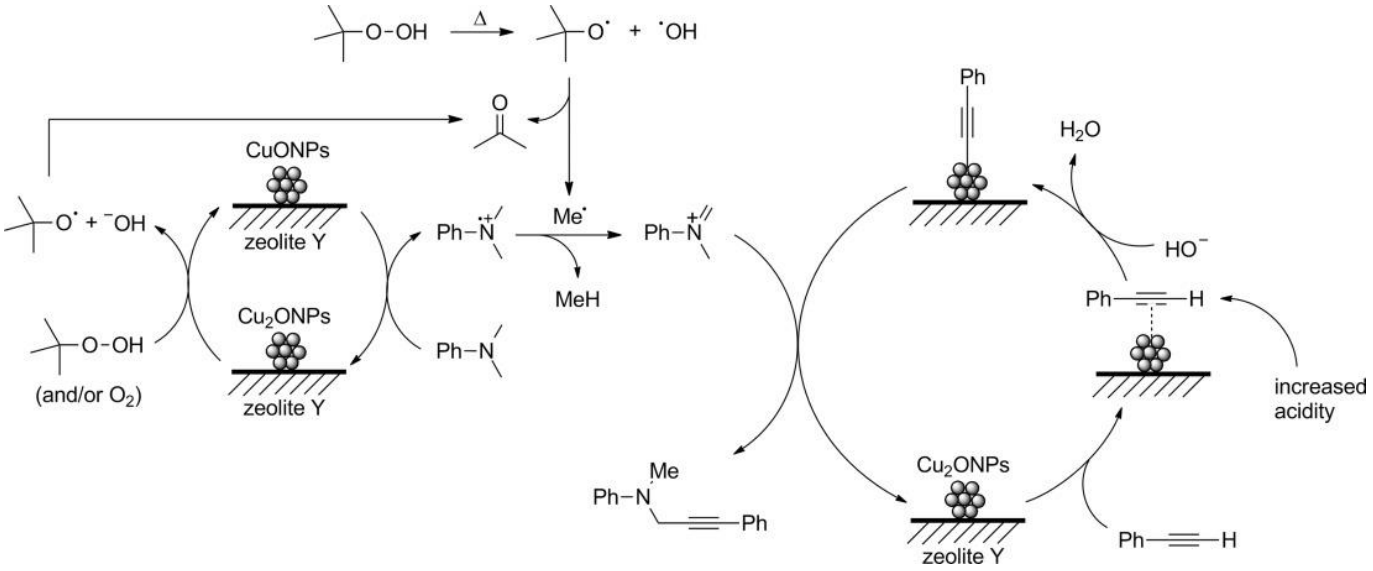

Fig. 11. Proposed mechanism for cross-dehydrogenative coupling of phenylacetylene and *N,N*-dimethylaniline catalysed by Cu-based nanoparticles supported on zeolite. Reproduced from [63] with permission of John Wiley and Sons and Copyright Clearance Center (license number: 5142910077768) 2015.

On the basis of all control tests, the authors proposed the mechanism represented in Fig. 11. The SET (Single Electron Transfer) and HAT (Hydrogen-Atom Transfer) sequence proposed seems to be the most plausible (more than the inverse one, HAT-SET), because no dimers arising from dimethylphenylamine radicals were detected.

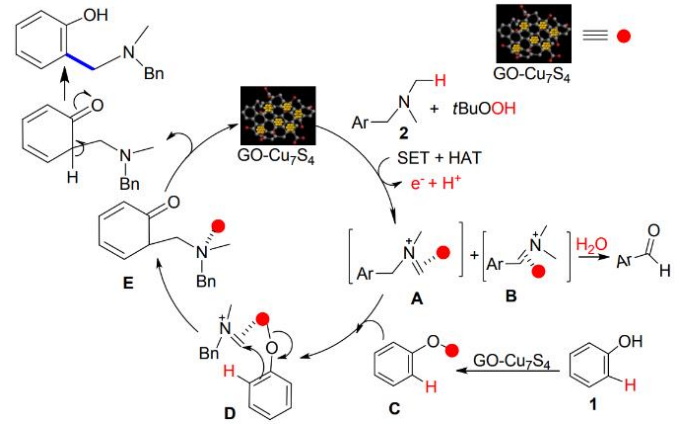

Fig. 12 Plausible radical mechanism for the Cu_7S_4 NPs on graphene oxide catalysed ortho-aminomethylation of phenol using TBHP as oxidising agent. Reproduced from [61b] with permission from the Royal Society of Chemistry.

Jain and co-workers have reported Cu_7S_4 NPs immobilised on graphene oxide applied in the *ortho*-aminomethylation of phenols through C(sp^2)–H-C(sp^3)–H CDC.[61b] Curiously, this reactivity was only observed using copper sulphides as catalytic precursors (including bulk materials such as CuS and Cu_2S); however, Cu_2O did not promote this transformation. Different control experiments, including the addition of radical scavenger (TEMPO) to the catalytic reaction, HR-MS and time-dependent ^{1}H NMR analyses of intermediates (evidencing the formation of an iminium cation) and the lack of reactivity when anisole was employed instead of phenol, permitted to the authors to propose a plausible surface-like pathway (Fig. 12).

Zero-valent copper nanoparticles (mean diameter 1.7 nm determined by TEM) synthesized under hydrogen atmosphere in glycerol, using PVP as stabiliser, and fully characterized (XPS and electrochemical studies proved the exclusive presence of Cu(0), together with the surface plasmon resonance evidenced by UV-vis; Fig. 13), were also efficiently applied in CDC reactions, leading to the synthesis of propargylamines from tertiary amines and terminal alkynes.[9a] When *N*-methylphenylaniline (a secondary amine) was used, *N*-methylation was also observed, indicating that TBHP acts as both methylating and oxidizing agent, in agreement with previous reported works by Phan, Truong and co-workers using copper ferrite and copper MOF as catalysts.[64] This catalytic system was also applied in the synthesis of propargylamines and *N*-containing heterocycles by A^3 (aldehyde, alkyne and amine) couplings. This catalyst was also active in KA^2 (ketone, alkyne and amine) couplings, taking into account that ketones are more reluctant than aldehydes in this type of three-component reactions (Scheme 7).

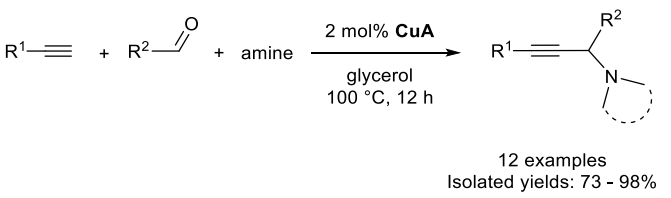

Scheme 7 Synthesis of propargylamines by A^3 coupling catalysed by preformed Cu(0) nanoparticles.[9a]

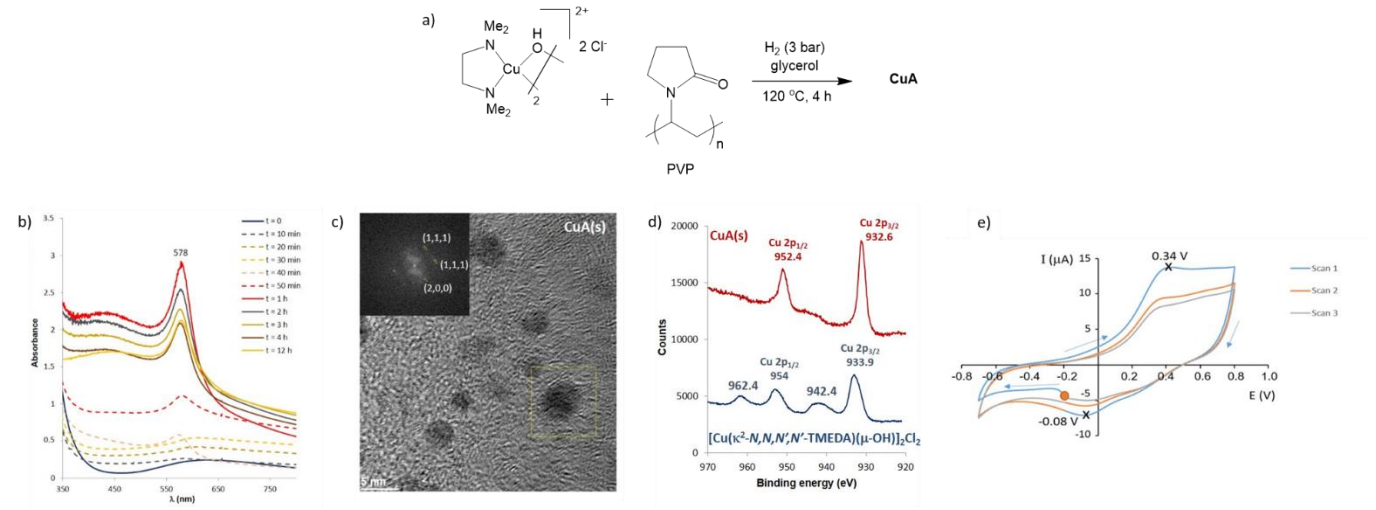

Fig. 13 a) Synthesis of Cu(0) NPs (**CuA**) prepared in glycerol; b) UV-vis spectra recorded at different times during the synthesis of **CuA**; c) HR-TEM micrograph of **CuA** including the crystallographic planes spots (Fast Fourier Transform from one selected nanoparticle); d) High-resolution XPS spectra at the Cu 2p binding energy region for **CuA** (red trace) and its precursor [Cu(κ²-*N,N,N′,N′*-TMEDA)(μ-OH)]$_2$Cl$_2$ (blue trace); e) Cyclic voltammetry of **CuA** in glycerol (the ornge dot indicates the starting point of the experiment). Adapted from 9a with permission of John Wiley and Sons and Copyright Clearance Center (license number: 5142920864622) 2017.

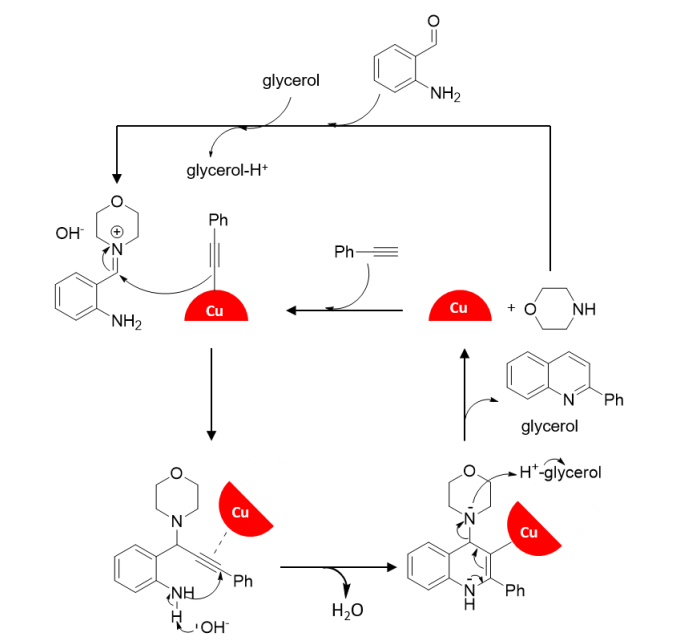

Fig. 14 Proposed mechanism for the synthesis of quinolones catalysed by zero-valent copper nanoparticles in glycerol, assisted by morpholine, via a tandem A^3 coupling/cycloisomerisaton process.[9a] Reproduced from 9a with permission of John Wiley and Sons and Copyright Clearance Center (license number: 5142920864622) 2017.

Copper is one of the most applied catalyst in theses multi-component transformations, but mainly using homogeneous species.[65] In the last decade, several nano-catalysts have been applied in this reactivity, but few of them using preformed copper-based nanoparticles; scarce mechanistic studies can be found.[66] Spectroscopic studies (IR and UV-vis) were carried with Cu(0) NPs in glycerol in the presence of phenylacetylene without observing the formation of Cu(I)-alkyne molecular species, even in the presence of morpholine. These data together with the negligible copper detected in the extracted organic compounds after catalysis (ICP-AES analyses), suggest that a copper surface-like reactivity takes place. Based on these observations, the authors suggested a plausible mechanism for the synthesis of heterocycles, where the alkyne is activated at the metal surface taking advantage of the electronic density of the nanoparticle then reacting with the iminium formed by condensation of the amine and aldehyde; the resulting propargylamine intermediate can give the cycloaddition promoted by the copper-alkyne interaction (Fig. 14). Alonso and co-workers proposed a similar mechanism for the synthesis of propagylamines catalysed by Cu_2O NPs supported on titania.[67]

4. C-heteroatom cross-couplings

The copper effect on C-heteroatom bond formation was first reported by Ullmann for the synthesis of diarylamines using super-stoichiometric amount of copper,[68] followed by the independent works of Ullmann[4] and Goldberg[5] reporting the first Cu-catalysed processes for the synthesis of bisaryl ethers and arylation of amines/amides, respectively.[69] As mentioned before, the high-energy demanding initial conditions employed in these transformations together with the relative low functional group tolerance, Cu-based catalysts were scarcely studied during the long decades. In the nineties, Buchwald[70] and Hartwig[71] independently applied homogeneous Pd-based catalysts in the synthesis of amines by coupling of aryl halides and primary or secondary amines; this methodology has been successfully applied including C-O and C-S cross-coupling reactions, proving the versatility of palladium catalytic systems.[72] With the aim of using more convenient catalysts, since 2000 copper, including heterogeneous systems in particular copper-based nanoparticles, have been largely developed for C-heteroatom bond formations.[8a, 73] In this section, the works involving Cu-based NPs catalysed hetero-

couplings with a special insight in the study of mechanisms are described.

4.1. C-N bond formation: cross-dehydrogenative couplings

As previously mentioned, CDC reactions represent a sustainable tool for synthetic purposes (see above section 3.4). In particular N-H/C-H CDC has emerged as an effective way for the synthesis of *N*-containing compounds, scaffolds present in many natural products and pharmaceutical compounds.[74]

In 2010, Li and co-workers reported for the first time the direct amidation of aryl pyridines by a Cu-catalysed oxidative C-N bond formation using di-*tert*-butyl peroxide as oxidant and CuBr as catalytic precursor, by activation of N-H and C-H bonds.[75] CuO nanoparticles on carbon nano-powder (two populations of particles observed by TEM with mean sizes of 10 and 27 nm) were applied in the synthesis of imines by both self-coupling of a large variety of amines and cross-coupling of primary amines and aniline, using air as oxidant (Fig. 15).[76] Wang and co-workers developed CuO nanoparticles supported on kaolin for the synthesis of quinazolines (Scheme 8).[77] The authors evidenced the leaking of CuO NPs from the support during the reaction, precluding an efficient recycling.

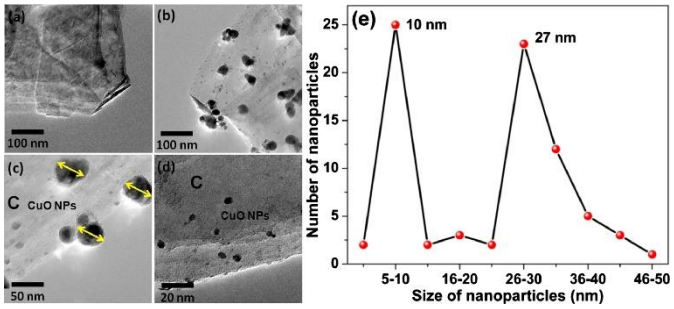

Fig. 15 TEM micrographs (a) Carbon nanopowder and (b, c and d) CuO NPs@Carbon nanopowder, and (d) size distribution histogram of CuO NPs. Reproduced from [76] with permission of Elsevier and Copyright Clearance Center (license number: 5160200537079) 2017.

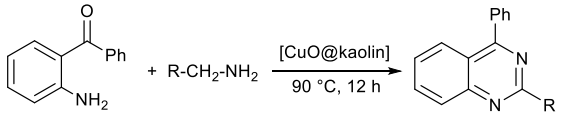

Scheme 8 Synthesis of quinazolines catalysed by CuO nanoparticles supported on kaolin.[77]

Phan and co-workers described CuO NPs supported on porous metal-organic framework for the synthesis of α-ketoamides through oxidative CDC of amines and α-carbonyl aldehydes under aerobic conditions (Scheme 9);[78] the authors postulated a heterogeneous catalytic pathway based on the control filtration test (after removing the catalyst, the solution did not progress towards the expected product under catalytic conditions and <10 ppm of Cu was detected in the filtrate by ICP-MS analysis) and an efficient recycling (the catalyst was reused up to 9 runs without activity loss).

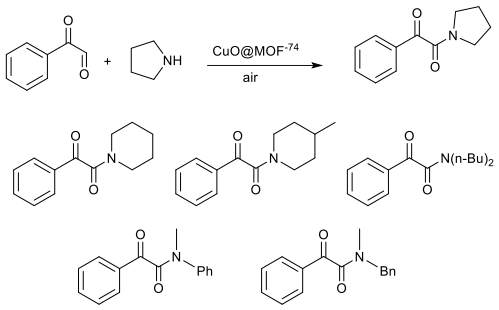

Scheme 9 CuO NPs on MOF catalysed the synthesis of α-ketoamides through oxidative CDC of aliphatic and aromatic amines with phenylglyoxal.[78]

From a mechanistic point of view, it is important to highlight the unsupported Cu_2S NPs stabilized by trioctylphosphine (mean diameter *ca*. 34 nm determined by TEM) applied in the oxidative amination of *N,N*-dimethylbenzylamines to lead to the formation of functionalized *N*-containing heterocyles (Scheme 10).[79]

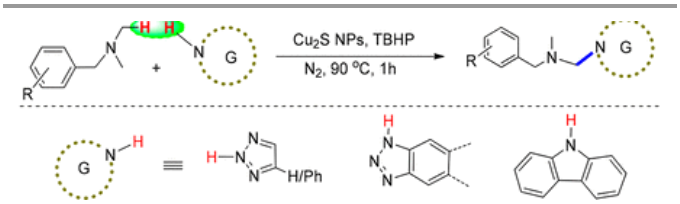

Scheme 10 Cu_2S catalysed oxidative amination of *N,N*-dimethylbenzylamines through CDC processes. Adapted with permission from [79]. Copyright 2018 American Chemical Society.

Several control experiments were carried out in order to elucidate the mechanism of these CDC reactions. It was proven the inhibitory effect of TEMPO pointing to the presence of radical intermediates. Furthermore, time-dependent EPR analyses of the catalytic mixture evidenced the formation of Cu(II) species and HR-MS analyses revealed the formation of iminium intermediates. Based on these data, the authors proposed the mechanism shown in Fig. 16. The yield decrease observed during the catalyst recycling (carried out up to 5 runs, yield after each consecutive run: 74-69-65-61-55%) was consistent with the agglomeration of Cu_2S nanoparticles after catalysis [mean size of nanoparticles: from *ca*. 30 nm (fresh catalyst) to *ca*. 45 nm (after 5 run) determined by TEM].

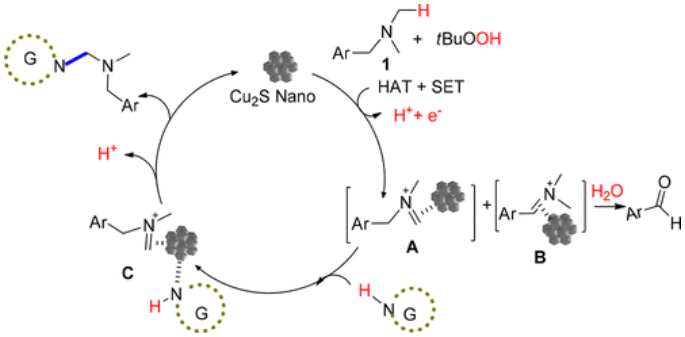

Fig. 16 Proposed pathway for oxidative amination of *N,N*-dimethylbenzylamines catalysed by Cu_2S nanoparticles. Reprinted with permission from [79]. Copyright 2018 American Chemical Society

4.2. C-N bond formation: Ullmann couplings

Cross-couplings between aryl halides and *N*-based reagents (anilines, amides…) catalysed by copper precursors have been extensively studied in the literature, mainly involving copper molecular species as catalytic precursors.[80] Due to the relative stability of copper species exhibiting different oxidation states (from Cu(0) to Cu(III)), both ionic (involving oxidative addition/reductive elimination steps) and radical (involving single electron transfer steps) mechanisms have been proposed based on different types of control experiments and theoretical calculations.[69]

In 2009, Sreedhar and co-workers reported for the first time the use of CuI NPs in C-N and C-O bond formation under ligand-free conditions.[81] The authors proposed a mechanism based on the CuI NPs stabilization by DMF and the amines and alcohols used as reagents. Hot filtration test (no reaction after catalyst removal from the catalytic solution at the first half of reaction time) and TEM analysis after several catalytic runs (catalyst did not exhibit changes in morphology) pointed to a surface-like reactivity (Fig. 17). They assumed that the cross-coupling proceeds by oxidative addition of the aryl halide at the nanoparticle surface promoted by electronic density sharing on neighbouring copper atoms.

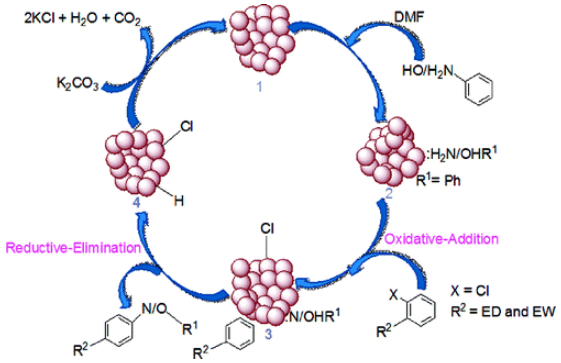

Fig. 17. Plausible mechanism for C-N and C-O bond formation in arylation processes. Reprinted with permission from [81]. Copyright 2009 American Chemical Society.

Later, Xu, Feng and co-workers reported the use of CuI NPs in the chemoselective synthesis of anilines, phenols and thiophenols in aqueous medium, using aryl halides (bromo and iodo derivatives) and n-tetrabutylammonium hydroxide as base.[82] In the presence of ammonia or sulphur, the corresponding anilines and thiophenols were obtained without observing the formation of the corresponding phenols.

In the last decade, several works have been described using as catalytic precursors well-defined CuO NPs, both unsupported and supported on solids, some of them containing mechanistic studies.[10f] Kavermbu and co-workers reported the *N*-arylation of benzimidazole using unsupported CuO NPs (mean size determined by TEM and PXRD: 6-8 nm) as catalyst,[83] showing up the activation of aryl fluorides (containing electron withdrawing groups) along with bromo and chloro derivatives. Authors proposed an ionic pathway without reporting experimental controls.

Ahamed, Sen, Islam and co-workers have reported the synthesis of unsupported CuO NPs (mean diameter *ca.* 5 nm) prepared in water in the presence of *Ocimum Sanctum* leaf extract, acting as both reducing agent (high content on polyphenols) and nanoparticles stabiliser.[84] The as-prepared catalytic material was applied in the *N*-arylation of a large variety of amides and aryl/styryl halides (iodo and bromide derivatives) (Fig. 18).

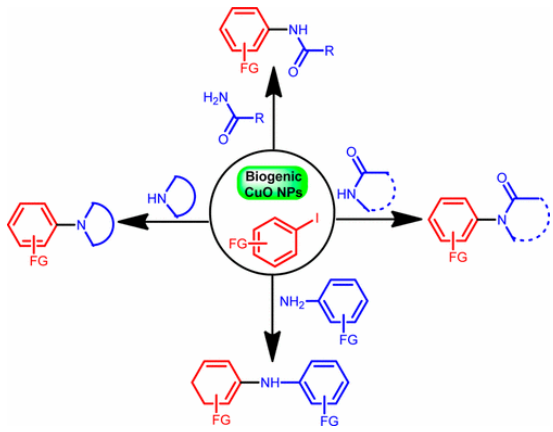

Fig. 18 CuO NPs catalysed C-N cross-couplings. Reprinted with permission from [84]. Copyright 2017 American Chemical Society.

The authors carried out some tests with the aim of obtaining inputs concerning the mechanism of these Cu-catalysed cross-couplings. Thus, the addition of a radical scavenger (TEMPO) did not influence on the catalytic reaction. Furthermore, when trans-styryl halides were used, the products showed full retention of configuration (presence of vinyl radical intermediates would lead to a mixture of stereoisomers).[85] These observations ruled out a radical pathway. Concerning copper, four-line hyperfine EPR spectra of the catalyst for fresh and intermediate stages, indicated the quantitative presence of Cu(II). Taking into account that the oxidative addition on Cu(II) seems quite doubtful, the authors proposed a mechanism consisting of a first coordination of the amide to Cu(II) metal centres (N-H activation) followed by a coordination of the aryl halide leading to a transient intermediate which evolves towards the C-X activation, forming the corresponding *N*-functionalized amide and the corresponding salt from the base (scavenger of HX) (Fig. 19).

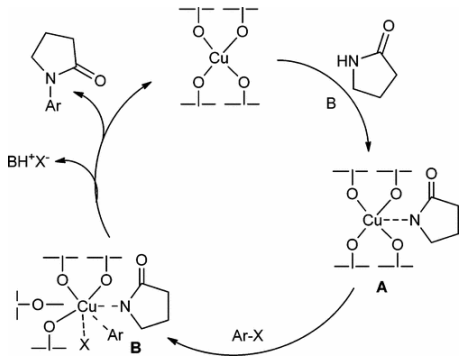

Fig. 19. Plausible mechanism for C-N and C-O bond formation in arylation processes. Reprinted with permission from [84]. Copyright 2017 American Chemical Society.

CuO NPs immobilised on silica (mean size of nanoparticles: *ca*. 30 nm) were efficiently applied in C-N cross-couplings of aryl halides (iodo, bromo and chloro derivatives) and various di-substituted amines (anilines, benzylamines, alkylamines).[86] The authors proposed a mechanism through oxidative addition/reductive elimination steps, assuming a prior reduction of CuO in the reaction medium probably promoted by the base (with formation of peroxides from KOH). CuO NPs supported on multi-walled carbon nanotubes (mean diameter of CuO NPs *ca.* 4.6 nm) were applied in the *N*-arylation of 2-phenylindoles.[87] From a mechanistic approach, the authors proposed a Cu(I)/Cu(III) heterogeneous mechanism, also presuming an *in situ* reduction of CuO in Cu(I) species (promoted by the base, in this case NaO*t*Bu). Cu_2O NPs supported on ascorbic acid coated magnetite (mean diameter in the range of 8-15 nm) were catalytically active for C-N (and also for C-O) cross-couplings, using aryl halides (iodo, bromo and chloro derivatives) and aniline, imidazole and alkyl primary amines.[88] The authors proposed a heterogeneous reactivity based on hot filtration tests and ICP analyses of the organic extracts. Cu_2O-based NPs were applied in the synthesis of diarylamines; the most active catalytic system was that constituted of a mixture of unsupported Cu(0) and Cu_2O NPs prepared by a polyol approach (1,3-propanediol used as solvent and reducing agent) from copper(II) acetate; the structure of the catalyst cannot be inferred from the reported characterization data (core-shell or mixture of independent Cu(0) and Cu(I) nanoparticles).[89] Cu(0) NPs supported on alumina/silica support were also active for the cross-couplings between aryl chlorides and *N*-heterocyclic and aromatic amines.[90] Patel and co-workers applied unsupported CuO NPs for the synthesis of a large panel of quinazolinones (31 examples, yields in the range 39-85%) through a sequential Ullmann coupling followed by intramolecular oxidative C-H amidation, affording better yields than when copper salts were used as catalytic precursors; after catalysis, TEM analyses evidenced catalyst agglomeration, in agreement with the inefficient recycling, results pointing to a plausible copper leaching during the reaction.[91]

4.3. C-N bond formation: Chan-Lam couplings

In 1998, Chan[92] and Lam[93] independently reported cross-couplings between aryl boronic acids and nitrogen-based nucleophiles, mediated by copper acetate and working under smooth conditions (often at room temperature). This methodology was quickly optimized and applied by several groups, becoming a valuable methodology for C-N bond formation,[94] mainly involving homogenous catalysts.[95]

Well-defined unsupported CuO NPs have been efficiently applied in *N*-arylation of imidazoles and anilines under mild conditions (methanol or methanol/water as solvent and temperatures in the range rt to 60 °C),[96] even working in the absence of added base.[96a] Moreover, supported Cu(0) nanoparticles on *N*-enriched graphene oxide found applications in the synthesis of diarylamines, suggesting a mechanistic pathway based on ligand exchange, followed by transmetallation, reductive elimination and oxidation; these elementary steps are proposed that occur at the metal surface of Cu(0) NPs immobilised on the graphene-based support and consequently excluding any metal leaching; unfortunately no mechanistic studies are described. Guo and co-workers reported a visible-light photocatalytic approach by Cu(0) NPs on graphene, taking advantage of the surface plasmon effect of the Cu NPs (Scheme 11).[97] This catalyst exhibited a relative high activity (TOF = 25.4 h^{-1}); working under optimized irradiation of 520-600 nm for the *N*-arylation of phenylboronic acid and imidazole; it was also efficient for the synthesis of diarylethers and dithioarylethers by C-O and C-S cross-coupling of arylboronic acids with phenols and thiophenol, respectively. The catalyst was characterized after being used in catalysis without observing any morphology change (TEM and powder XRD analyses); XPS evidenced a slight shift on the binding energy of Cu $2p_{3/2}$ pointing to the formation of Cu(I) species. The catalyst showed good recyclability up to the fifth run; after that, the catalytic activity was recovered by treatment of the catalyst under H_2 atmosphere. The catalytic behaviour observed for Cu NPs@graphene together with the catalyst characterisation (before and after reaction) strongly point to a surface reactivity.

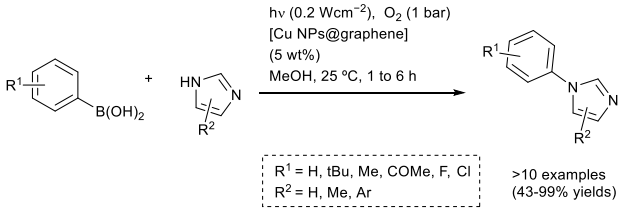

Scheme 11 Cu NPs@graphene catalysed Chan-Lam *N*-arylation of imidazole derivatives and arylboronic acids under visible light irradiation.[97]

4.4. C-N bond formation: alkyne-azide cycloaddition

Certainly, azide-alkyne cycloadditions (AAC) represent one of the most fruitful applications of copper-catalysed organic reactions, which belong to the transformations named "click chemistry".[98]

The effect of copper in AAC (1,3-dipolar cycloadditions firstly described by Huisgen in 1963 under metal-free conditions and thus leading to mixture of regioisomers),[99] was independently reported by Meldal[100] and Sharpless[101] in 2002. Since then, the regioselective synthesis of 1,4-disubstituted 1,2,3-triazoles has found worthy applications in different areas (drug design, macromolecules, biochemistry, materials).[102] Despite this vast scope and range of conditions and solvents, both aprotic and protic ones including water, mechanistic studies continue being of interest from a fundamental point of view.

Cu-based NPs have been applied in AAC processes, in many cases without concluding if the nanoparticles operate as true catalyst (surface reactivity) or as reservoir of molecular catalytically active species. One of the first reported works proving a heterogeneous reactivity was that published by Moores and co-workers using CuFe bimetallic magnetic nanoparticles constituted by a Fe(0) core and a Cu(I) shell; this conclusion was based on ICP-OES analyses of the catalytic solutions after catalyst removal, and catalyst recycling (up to 5

times) under inert conditions (in the presence of air, copper oxides are assumed to be formed, justifying the dramatic activity decrease).[103] Scaiano and co-workers studied the catalytic nature of copper species by single-molecule studies by Total Internal Reflection Fluorescence Microscopy (TIRFM), using well-defined Cu_2O NPs as catalytic precursors, both colloidal and supported systems (MCM-41 used as support)[98b]. Authors proved that the as-prepared NPs were able to catalyse the AAC on mole and single-molecule scales, in this latter case monitored by TIRFM involving Förster Resonance Energy (FRET) activation via formation of the corresponding triazoles that contain donor-acceptor dyes in close proximity. These single-molecule studies proved that the reaction initially proceeds through the formation of Cu-acetylides on the nanoparticle surface followed by azide attack, without copper ion leaching from the NPs.

Gómez and co-workers reported the synthesis of Cu_2O NPs stabilised by PVP and immobilised in glycerol (mean diameter: 4.7 nm), being a versatile catalyst for the synthesis of a wide panel of triazole-containing compounds, including one-pot AAC/C-N cross-coupling tandem processes.[104] The catalyst was recycled up to ten runs without evidencing activity loss, pointing to a surface reactivity. The same group evidenced the formation of CuI NPs in glycerol using CuI salt as catalytic precursor in the presence of long-alkyl-chain amines (such as oleylamine). In the absence of these amines, no formation of nanoparticles was observed and the amine-free CuI/glycerol system was not catalytically active, proving the crucial role of the Cu(I)-based nanoparticles.[105]

Alonso, Yus and co-workers prepared Cu-based NPs on active carbon (mean diameter: ca. 6 nm) constituted of Cu_2O and CuO NPs and efficiently applied in multi-component synthesis of β-hydroxy-1,2,3-triazoles from epoxides, alkynes and sodium azide in water (Fig. 20).[106] Deuteration control experiments evidenced the formation of Cu-acetylide intermediates, probably at the surface of the catalyst.

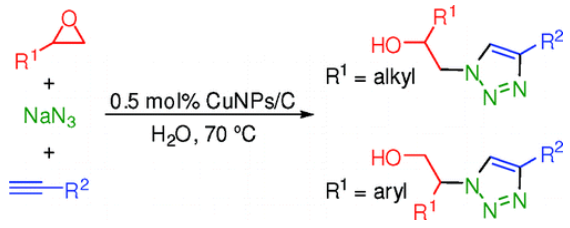

Fig. 20 Multicomponent synthesis of 1,4-disubstituted 1,2,3-triazoles catalysed by Cu_2O/CuO nanoparticles supported on activated carbon. Reprinted with permission from [106]. Copyright 2011 American Chemical Society.

Cu_2O nanocrystals showing different morphologies (nanocubes, octahedra, rhombic dodecahedra) were applied in the synthesis of drugs, proving that Cu_2O rhombic dodecahedra bounded by [110] facets were the most efficient for a wide range of reagents.[107]

Cu_3N NPs, also constituted of Cu(I) as Cu_2O based materials, found applications in AAC, working under smooth conditions (room temperature, from 12 h to 2 days).[108]

Cu(0)[109] and Cu(II) based NPs[110] have been also efficiently used as catalytic precursors for AAC, without evidences of the corresponding pathways, which probably generate Cu(I) intermediate species under catalytic conditions.

4.5. C-P bond formation

Alkynylphosphonates exhibit an increased interest due to the phosphonic functional group (acid or ester) present in natural and synthetic bioactive compounds.[111] Moglie and co-workers described the straightforward synthesis of alkynylphosphonates via cross-coupling between terminal alkynes and H-phosphonates catalysed by commercial Cu_2O, under base-free conditions and avoiding the use of moisture-sensitive reagents (such as metal acetylides and phosphonic halides).[112] Later on, Lu and co-workers used well-defined copper-based NPs immobilised on Nb_2O_5.[113] The full characterization of the catalytic material revealed that the metal nanoparticles are mainly constituted of Cu_2O together with Cu(0) (XPS analysis), very well-dispersed on the support (TEM analysis) exhibiting a mean size of 3.5 nm. Compared with other supports (such as ZrO_2, SiO_2, Al_2O_3), Nb_2O_5 gave the highest catalytic activity, depending on the nature of the solvent. The authors suggested that this catalytic behaviour can be attributed by the strong adsorption of diethylphosphite on Nb_2O_5 due to its Lewis acid nature (FT-IR controls). Concerning the copper sites, the requirement of oxygen to lead to an efficient coupling seems to point that Cu(I) sites are the catalytic centers and a Cu(I)/Cu(II) mechanism seems to operate. Taking into account that no alkyne homocoupling was detected, Cu-phosphonate intermediates were probably formed instead of copper-alkynyl ones. Hot filtration experiment pointed to a surface-like catalytic reactivity. Based on these experimental evidences, a cross-coupling alkyne/H-phosphonate pathway was proposed (Fig. 21).

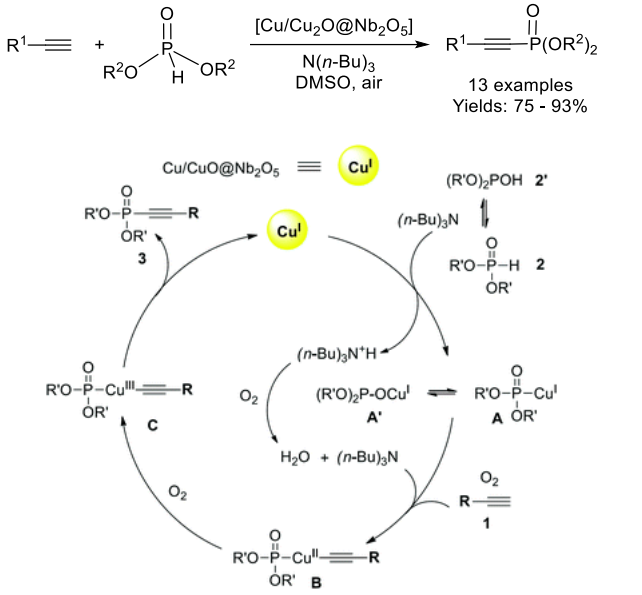

Fig. 21 Scope of the cross-coupling between phosphite esters Cu-based nanoparticles immobilised on Nb_2O_5 (top) and a proposed mechanism for this coupling (bottom). Adapted from [113] with permission from the Royal Society of Chemistry.

4.6. C-O, C-S and C-Se bond formation

Building C-heteroatom bonds, in particular C-N, C-O and C-S bonds, represents a prevailing approach in the synthesis of polymers, natural products and fine chemicals. One of the most classical methodologies is the copper-promoted Ullmann couplings.[52b, 69, 80, 114] Catalytic systems working at moderate temperatures have been developed, reducing both energy consumption and waste production (low E-factor). Among them, Cu-based nanomaterials have led to efficient processes for the production of ethers, amines and thioethers.[10f, 73, 115].

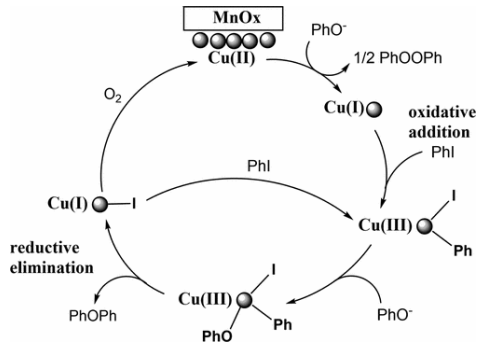

Fig. 22 Plausible pathway for Ullmann coupling reactions catalysed by CuO nanoparticles supported on MnO_x. Reprinted with permission from [116]. Copyright 2017 American Chemical Society

From a mechanistic point of view, it is important to highlight the contribution of Suib, Angeles-Boza and co-workers applying CuO nanoparticles supported on mesoporous MnO_x to the formation of C-O, C-N and C-S bonds by coupling between iodo-aryls and phenols, aromatic *N*-based reagents and thiophenol.[116] This catalytic material was less active in the presence of *N*- and *S*-based reagents probably due to the stronger coordination to the copper sites than phenols, but still showing an important reactivity; in other words, the poisoning absence using aniline, imidazoles or thiophenol in Ullmann-type couplings was also observed using CuO nanoparticles synthesized from Cu(II)-Cu(I) mixed-valence polymer[117] and unsupported CuO NPs.[118] With the purpose of proving that Cu(I) species are the catalytically active sites, a Cu(II)-based catalyst on TiO_2 was prepared (instead of MnO_x, in order to avoid the copper oxidation by the support), evidencing by XPS the formation of Cu(I) after the reaction with phenol under N_2. The catalytic reactivity observed using Cu_2O@graphene[119] or Cu_2O@TiO_2 as catalysts[120] for the coupling of halo-arenes with phenols corroborates the requirement of Cu(I) species. Accordingly, CuO@MnO_x should be reduced by the reagent with the concomitant formation of the corresponding peroxide or disulfide. Moreover, the control experiment using a radical scavenger (phenotriazine) ruled out the presence of radical intermediates. From kinetic studies, the Hammet analysis pointed to an oxidative addition of the aryl iodide to Cu(I) (ρ = +1.0) and a coordination of the phenol to Cu(I) (ρ = -2.9), by comparison with Rh(I),[121] Ni(0)[122] and Pd(0)[123] homogenous catalysts. Reported mechanistic studies using homogeneous catalysts proved that oxidative addition takes place prior to the nucleophilic addition.[124] Furthermore, the heterogeneous nature of the catalyst was proven by the lack of copper leaching in a hot filtration experiment. Based on these experimental results, including DFT calculations, the authors proposed a Cu(I)/Cu(III) pathway (Fig. 22). As proposed by Sreedhar and co-workers for C-O and C-N couplings, the presence of a base (such as K_2CO_3) acts as HX scavenger adsorbed on Cu-based nanoparticles.[81]

Other than Cu(II)- and Cu(I)-based catalysts, Cu(0)-nanocatalysts have been also applied in Ullmann-type couplings. Obora and co-workers prepared colloidal Cu(0) NPs in DMF under surfactant-free conditions.[125] Their characterization proved that the as-prepared zero-valent CuNPs (mean diameter *ca*. 2 nm, determiner by TEM) were capped by a copper oxide shell (XPS analysis). This catalytic system was active for the synthesis of diaryl ethers, from both bromo- and iodo-arene reagents. Cu(0)NPs immobilised on nafion-graphene nanoribbons, exhibiting a mean size of *ca*. 26 nm (determined by TEM and PXRD), were successfully applied in a wide-ranging scope of aryl halides (iodo- and bromo-based substrates) and phenols,[126] under both base- and oxygen-free conditions. Kassaee and co-workers prepared Cu(0)NPs immobilised on Fe_3O_4 nanoparticles decorated by chitosan, from $CuCl_2$ in the presence of the support using hydrazine hydrate as reducing agent.[127] This catalyst was active for a large variety of phenols and iodo-aryls. The authors proposed a Cu(0)/Cu(II) pathway, but no mechanistic studies are described. In addition, Sharma, Gawande and co-workers reported a magnetically retrievable catalyst nanocomposite made of Cu(0) and maghemite exhibiting excellent catalytic activities towards C–O and C–S bond-formation reactions and reusability.[128] XPS, TEM and high-angle annular dark-field scanning transmission electron microscopy with energy-dispersive spectroscopy atomic absorption spectroscopy were used for the full characterization of the nanocatalyst (Fig. 23).

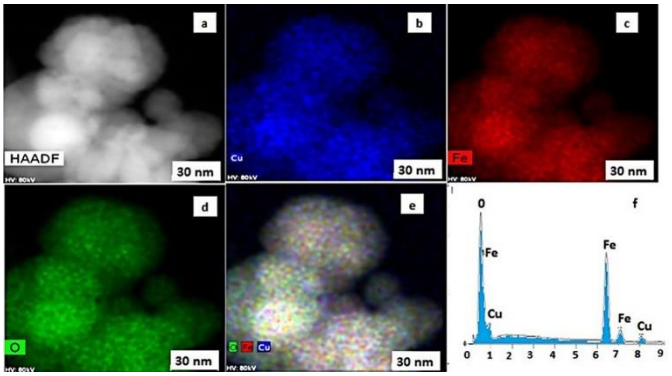

Fig. 23 HAADF-STEM images of Cu-maghemite nanocatalyst; a) HAADF image; b) Distribution of Cu by HAADF; c) Distribution of Fe by HAADF; d) Distribution of O by HAADF; e) Distribution of Cu, Fe, and O together by HAADF; f) EDS spectrum indicating the presence of Cu. Reprinted from [128] with permission of John Wiley and Sons and Copyright Clearance Center (license number: 5160250578857) 2015.

Thorough mechanistic insights using a catalyst composite made of ultra-small Cu NPs of 1–2 nm embedded in a matrix of chitosan microspheres have been recently reported by García and co-workers for the synthesis of diaryl sulphides from

thiophenol and iodoaryls (or bromo- and chloroaryls bearing electron withdrawing groups).[10b]

This nanocatalyst system was prepared in a stepwise manner consisting of solvothermal reduction of $Cu(NO_3)_2$ in ethylene glycol at 150 °C (polyol reduction method), affording Cu NPs, which were then supported on chitosan via hydrogel formation under acidic media, followed by microsphere precipitation with a NaOH solution.[10b] Detailed XPS characterization of the fresh catalysts and after reaction revealed the loss of nitrogen content of the chitosan matrix as well as the presence of Cu in low oxidation states, probably Cu(I) and Cu(0). Although the overall concentration of surface Cu atoms remains unchanged after reaction, the contribution of Cu 2p peak at 931.5 eV and the observation of the Auger peak at 916.5 eV evidence the implication of Cu(I) as active catalyst. The authors proposed two concomitant surface processes on low valent copper atoms: on the one hand, a multiatomic oxidative addition of the aryl halide substrate, as well as the coordination of the thiophenolate anion leading to a reductive elimination of the corresponding diphenyl sulfide product (Fig. 24).[10b] Not only the oxidative addition is easier for aryl iodides in comparison to bromides and chloride counterparts, but also the weaker binding energy of the concomitant copper halide species (Cu-Cl > Cu-Br > Cu-I) may preclude deleterious catalyst passivation pathways. In particular, the binding energy of the concomitant copper halide species (Cu-Cl > Cu-Br > Cu-I) has been identified as a key parameter in the optimization of catalytic processes due to its relevance in terms of both the leaching of molecular copper species and catalyst poisoning. Despite moderate activity decrease after the first run, the catalytic activity of the recycled catalyst remains consistently stable after 5 runs.[10b] Moreover, spherical Cu_2O nanocatalysts (4.7 ± 1.5 nm mean size) immobilised in glycerol have also exhibited excellent selectivity and conversions towards unsymmetrical diaryl sulphides and alkyl aryl sulphides from thiols and aryl iodides.[104]

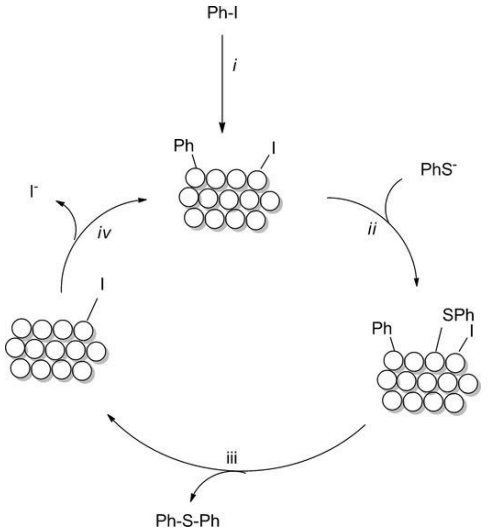

Fig. 24 Simplified mechanistic proposal for C–S cross-coupling on Cu NPs. i) Ph–I cleavage on low-coordinated surface Cu sites; ii) Adsorption of thiophenoalete on the surface; iii) PhSPh desorption; iv) Iodide desorption. Reprinted from [10b] with permission of John Wiley and Sons and Copyright Clearance Center (license number: 5143520480932) 2015.

Despite the good reaction selectivity towards unsymmetrical diaryl sulphides obtained with nanocatalyst composites of Cu NPs (2-3 nm in size) immobilised on hexagonal microporous silica, the formation of disulphides via oxidative homocoupling was also identified as reported by Luque, Macquarrie and co-workers.[129] The heterogeneity in copper oxidation states of the catalyst could be responsible of the different selectivity outcomes, namely 60% of the copper content corresponded to Cu(0) (XPS peak centred at 931.8 eV), together with Cu(I) and Cu(II) oxidation states (at 934.1 and 942.2 eV, respectively).

However, alternative reaction manifolds may be possible for Cu(II) nanocatalysts to enable Ullmann-type C-S cross coupling reactions as reported by Wang and co-workers for a catalyst system made of CuO nanoparticles (12.6 ± 3 nm of size determined by TEM, 2p3/2 and 2p1/2 XPS peaks 934.8 and 955 eV) immobilised on mesoporous nitrogen-doped carbon materials of high specific surface areas (from 373 to 488 m^2 g^{-1}), as the oxidative reaction conditions using DMSO at 100 °C may preclude potential contributions of low-valent Cu species in such transformation.[130] Analogous results in DMSO have been obtained with a catalyst nanocomposite featuring spherical CuO nanoparticles (55 ± 15 nm diameter) supported on graphene oxide (Fig. 25).[10d]

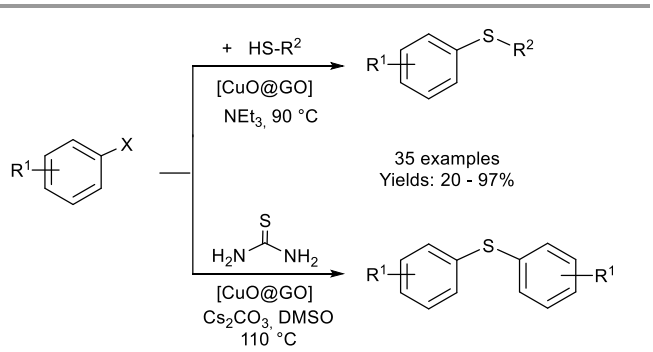

Fig. 25 Synthesis of aryl sulphides catalysed by CuO NPs@ graphene oxide (GO).[10d]

The use of telescoped processes for the synthesis of symmetrical and unsymmetrical diaryl sulfides has also been achieved with CuO nanocatalysts with thiourea as an effective sulfur surrogate and aryl iodides substrates in DMSO as solvent.[131] However further mechanistic insights taking into account the thiophilicity of copper nanocatalysts and their role in the cascade reactions needs to be further studied. Thus far, literature reports by Kakulapati and co-workers on the synthesis of diarylsulfides and alkylarylsulfides from iodo- and bromoaryls with ethyl potassium xanthogenate and a commercial CuO nanocatalyst system (<50 nm) not only identified the leaching of copper species by ICP-AES (0.8 and 1.2 ppm after first and second run), but also demonstrated the negligible role in catalysis of such molecular species in catalysis upon removal of CuO nanoparticles.[132]

Recent results on the encapsulation of CuO nanoparticles inside metal-organic frameworks (MOF) point out the relevance of structural confinement towards the preparation of size defined copper nanoparticles featuring a superficial layer of CuO from 2.1 ± 0.6 nm to 4.4 ± 0.9 nm, depending on the preparation

conditions.[133] The as-prepared MOF embedded catalytic systems showed excellent activity towards the formation of diaryl sulphides via C-S cross-coupling reactions and was reused up to four times without nanoparticle aggregation. These results shed light on the active role of metal nanoparticle systems and their oxides to enable substrate activation via surface mechanisms.

Despite the fact that C-Se cross coupling reactions have been less explored with nanocatalytic systems, a few reports on CuO nanoparticle catalytic systems (up to 40 nm) with selenourea[134] or *N*,*N*-diethyl selenoformamide[135] their use towards the synthesis of diaryl selenides and diaryl diselenides, the latter being a reaction intermediate in the synthesis of the former via the cleavage of the Se-Se bond as decribed by Rama Rao and co-workers with analogous CuO nanocatalysts under basic conditions.[136]

5. Summary and outlook

This review considers reported contributions related to monometallic copper-based nanocatalysts applied in organic synthesis, in particular in coupling reactions, which contribute to rationalise the catalytic behaviour observed in this multifaceted reactivity.

Advances on operando techniques (so far more developed for homogeneous catalytic processes) adapted to coupling reactions involving metal nanoparticles under catalytic conditions, represent a foremost challenge for evidencing metal-reagent interactions and intermediates (such as the work developed by Scaiano's team)[98b] by a straightforward way, together with theoretical approaches taking into account the simultaneous presence of different reagents and additives, other than solvents.

Given the versatility in structure and oxidation states ranging from zero-valent to Cu(III) species, the development of Cu-based catalytic systems capable to selectively enable one- or two-electron processes shall be key for the rational design of efficient nanocatalytic systems towards sustainable applications.

Author Contributions

The authors have equally contributed to the writing of this review.

Conflicts of interest

The authors declare that there is no conflict of interest.

Acknowledgements

The Centre National de la Recherche Scientifique (CNRS) and the Université Toulouse 3 – Paul Sabatier are gratefully acknowledged for their financial support. M. C. thanks the Ministère de l'Enseignement Supérieur et de la Recherche of the French government for a PhD scholarship.

Notes and references

1. A. Wurtz, *Justus Liebigs Ann. Chem.*, 1855, **96**, 364-375.
2. C. Glaser, *Ber. Dtsch. Chem. Ges.*, 1869, **2**, 422-424.
3. F. Ullmann and J. Bielecki, *Ber. Dtsch. Chem. Ges.*, 1901, **34**, 2174-2185.
4. F. Ullmann and P. Sponagel, *Ber. Dtsch. Chem. Ges.*, 1905, **38**, 2211-2212.
5. I. Goldberg, *Ber. Dtsch. Chem. Ges.*, 1906, **39**, 1691-1692.
6. For recent reviews, see: a) S. Mondal, *ChemTexts*, 2016, **2**, 17 (11 pages); b) K. S. Sindhu and G. Anilkumar, *RSC Adv.*, 2014, **4**, 27867-27887; c) S. Thapa, B. Shrestha, S. K. Gurung and R. Giri, *Org. Biomol. Chem.*, 2015, **13**, 4816-4827; d) L.-C. Campeau and N. Hazari, *Organometallics*, 2019, **38**, 3-35.
7. a) U. Heiz and U. Landman, *Nanocatalysis*, Springer, Berlin, 2007; b) M. H. G. Prechtl, *Nanocatalysis in Ionic Liquids*, Wiley-VCH, Weinheim, 2017 ; c) F. Valentini, G. Brufani, L. Latterini and L. Vaccaro, in *Advanced Heterogeneous Catalysts Volume 1: Applications at the Nano-Scale*, American Chemical Society, 2020, vol. 1359, ch. 17, pp. 513-543; d) U. Heiz and U. Landman, *Nanocatalysis*, Springer Berlin, Heidelberg, 2007; p 191; e) M. Camats, D. Pla and M. Gómez, in *Recent Advances in Nanoparticle Catalysis*, eds. P. W. N. M. van Leeuwen and C. Claver, Springer International Publishing, 2020, pp. 249-280.
8. a) M. Nasrollahzadeh, F. Ghorbannezhad, Z. Issaabadi and S. M. Sajadi, *Chem. Rec.*, 2019, **19**, 601-643; b) M. B. Gawande, A. Goswami, F.-X. Felpin, T. Asefa, X. Huang, R. Silva, X. Zou, R. Zboril and R. S. Varma, *Chem. Rev.*, 2016, **116**, 3722-3811; c) R. B. Nasir Baig, M. N. Nadagouda and R. S. Varma, *Coord. Chem. Rev*, 2015, **287**, 137-156.
9. a) T. Dang-Bao, C. Pradel, I. Favier and M. Gómez, *Adv. Synth. Catal.*, 2017, **359**, 2832-2846; b) I. Favier, D. Pla and M. Gómez, *Catal. Today*, 2018, **310**, 98-106.
10. a) J. F. Blandez, A. Primo, A. M. Asiri, M. Alvaro and H. Garcia, *Angew. Chem. Int. Ed.*, 2014, **53**, 12581-12586; b) S. Frindy, A. El Kadib, M. Lahcini, A. Primo and H. Garcia, *ChemCatChem*, 2015, **7**, 3307-3315; c) S. Frindy, A. El Kadib, M. Lahcini, A. Primo and H. Garcia, *Catal. Sci. Technol.*, 2016, **6**, 4306-4317; d) A. Kamal, V. Srinivasulu, J. N. S. R. C. Murty, N. Shankaraiah, N. Nagesh, T. Srinivasa Reddy and A. V. Subba Rao, *Adv. Synth. Catal.*, 2013, **355**, 2297-2307; e) A. R. Rosario, K. K. Casola, C. E. S. Oliveira and G. Zeni, *Adv. Synth. Catal.*, 2013, **355**, 2960-2966; f) B. C. Ranu, R. Dey, T. Chatterjee and S. Ahammed, *ChemSusChem*, 2012, **5**, 22-44; g) J. Huang, D. Lu and T. Mandal, *Synth. Commun.*, 2021, **51**, 1923-1946.
11. T. S. Rodrigues, A. G. M. da Silva and P. H. C. Camargo, *J. Mater. Chem. A*, 2019, **7**, 5857-5874.
12. L. Piccolo, *Catal. Today*, 2021, **373**, 80-97.
13. R. Cheula, M. Maestri and G. Mpourmpakis, *ACS Catal.*, 2020, **10**, 6149-6158.
14. J. Yan, B. K. Teo and N. Zheng, *Acc. Chem. Res.*, 2018, **51**, 3084-3093.
15. C. Glaser, *Justus Liebigs Ann. Chem.*, 1870, **154**, 137-171.
16. a) A. S. Hay, *J. Org. Chem.*, 1960, **25**, 1275-1276; b) A. S. Hay, *J. Org. Chem.*, 1962, **27**, 3320.
17. F. Nador, L. Fortunato, Y. Moglie, C. Vitale and G. Radivoy, *Synthesis*, 2009, **23**, 4027-4031.
18. F. Nador, M. A. Volpe, F. Alonso, A. Feldhoff, A. Kirschning and G. Radivoy, *Appl. Catal., A*, 2013, **455**, 39-45.

19. F. Alonso, T. Melkonian, Y. Moglie and M. Yus, *Eur. J. Org. Chem.*, 2011, **13**, 2524-2530.
20. C. Gonzalez-Arellano, A. M. Balu, R. Luque and D. J. MacQuarrie, *Green Chem.*, 2010, **12**, 1995-2002.
21. D. Chakraborty, S. Nandi, D. Mullangi, S. Haldar, C. P. Vinod and R. Vaidhyanathan, *ACS Appl. Mater. Interfaces*, 2019, **11**, 15670-15679.
22. B.-X. Tang, X.-N. Fang, R.-Y. Kuang, J.-H. Wu, Q. Chen, S.-J. Hu and Y.-L. Liu, *Appl. Organomet. Chem.*, 2016, **30**, 943-945.
23. A. V. Zuraev, Y. V. Grigoriev, L. S. Ivashkevich, A. S. Lyakhov and O. A. Ivashkevich, *Z. Anorg. Allg. Chem.*, 2017, **643**, 1215-1219.
24. S. T. Aziz and R. U. Islam, *Catal. Lett.*, 2018, **148**, 205-213.
25. H. Xu, L. Wu, J. Tian, J. Wang, P. Wang, X. Niu and X. Yao, *Eur. J. Org. Chem.*, 2019, **2019**, 6690-6696.
26. D. I. Gordeychuk, V. N. Sorokoumov, V. N. Mikhaylov, M. S. Panov, E. M. Khairullina, M. V. Melnik, V. A. Kochemirovsky and I. A. Balova, *Chem. Eng. Sci.*, 2020, **227**, 115940.
27. J. Jover, *J. Chem.*, 2015, 430358/430351.
28. a) G. Eglinton and A. R. Galbraith, *Chemistry & Industry*, 1956, **28**, 736–737; b) G. Eglinton and A. R. Galbraith, *J. Chem. Soc.*, 1959, 889-896.
29. F. Bohlmann, H. Schönowsky, E. Inhoffen and G. Grau, *Chem. Ber.*, 1964, **97**, 794-800.
30. a) N. Barot, S. B. Patel and H. Kaur, *J. Mol. Catal. A: Chem.*, 2016, **423**, 77-84; b) L. Al-Hmoud, S. Bali, S. Mahamulkar, J. Culligan and C. W. Jones, *J. Mol. Catal. A: Chem.*, 2014, **395**, 514-522; c) S. Biswas, K. Mullick, S.-Y. Chen, D. A. Kriz, M. D. Shakil, C.-H. Kuo, A. M. Angeles-Boza, A. R. Rossi and S. L. Suib, *ACS Catal.*, 2016, **6**, 5069-5080; d) N. Sgrolli, N. Imlyhen, J. Volkman, A. M. Raspolli-Galletti and P. Serp, *Mol. Catal.*, 2017, **438**, 143-151.
31. H. Zhao, G. Mao, H. Han, J. Song, Y. Liu, W. Chu and Z. Sun, *RSC Adv.*, 2016, **6**, 41108-41113.
32. G. Cheng and M. Luo, *Eur. J. Org. Chem.*, 2011, **13**, 2519.
33. Y. Moglie, E. Mascaró, F. Nador, C. Vitale and G. Radivoy, *Synth. Commun.*, 2008, **38**, 3861-3874.
34. A. A. Ponce and K. J. Klabunde, *J. Mol. Catal. A: Chem.*, 2005, **225**, 1-6.
35. N. Candu, A. Simion, S. M. Coman, A. Primo, I. Esteve-Adell, V. I. Parvulescu and H. Garcia, *Top. Catal.*, 2018, **61**, 1449-1457.
36. R. T. Addanki Tirumala, A. P. Dadgar, F. Mohammadparast, S. B. Ramakrishnan, T. Mou, B. Wang and M. Andiappan, *Green Chem.*, 2019, **21**, 5284-5290.
37. P. K. Raul, A. Mahanta, U. Bora, A. J. Thakur and V. Veer, *Tetrahedron Lett.*, 2015, **56**, 7069-7073.
38. a) N. Kirai and Y. Yamamoto, *Eur. J. Org. Chem.*, 2009, **12**, 1864; b) P. Puthiaraj, P. Suresh and K. Pitchumani, *Green Chem.*, 2014, **16**, 2865-2875; c) A. S. Demir, O. Reis and M. Emrullahoglu, *J. Org. Chem.*, 2003, **68**, 10130-10134.
39. X.-F. Wu, P. Anbarasan, H. Neumann and M. Beller, *Angew. Chem., Int. Ed.*, 2010, **49**, 9047-9050.
40. For selected reviews, see: a) Z. Wang, C. Wan and Y. Wang, in *Copper-Mediated Cross-Coupling Reactions*, eds. G. Evano and N. Blanchard, 2013, pp. 745-784; b) I. P. Beletskaya and A. V. Cheprakov, *Coord. Chem. Rev.*, 2004, **248**, 2337-2364.
41. For selected reviews, see: a) W. Shi and A. Lei, *Tetrahedron Lett.*, 2014, **55**, 2763-2772; b) J. Liu, J. W. Y. Lam and B. Z. Tang, *Chem. Rev.*, 2009, **109**, 5799-5867.
42. For selected contributions, see: a) B. S. Navale and R. G. Bhat, *RSC Adv.*, 2013, **3**, 5220-5226; b) H. Xu, K. Wu, J. Tian, L. Zhu and X. Yao, *Green Chem.*, 2018, **20**, 793-797; c) B. Lai, R. Bai and Y. Gu, *ACS Sustainable Chem. Eng.*, 2018, **6**, 17076-17086.
43. R. Sarkar, A. Gupta, R. Jamatia and A. K. Pal, *Appl. Organomet. Chem.*, 2020, **34**, e5646.
44. For selected reviews, see: a) R. Chinchilla and C. Najera, *Chem. Soc. Rev.*, 2011, **40**, 5084-5121; b) Y. N. Kotovshchikov, G. V. Latyshev, N. V. Lukashev and I. P. Beletskaya, *Org. Biomol. Chem.*, 2015, **13**, 5542-5555; c) F. Mohajer, M. M. Heravi, V. Zadsirjan and N. Poormohammad, *RSC Adv.*, 2021, **11**, 6885-6925; d) I. Kanwal, A. Mujahid, N. Rasool, K. Rizwan, A. Malik, G. Ahmad, S. A. A. Shah, U. Rashid and N. M. Nasir, *Catalysts*, 2020, **10**, 443.
45. For a recent review, see: F. Mohjer, P. Mofatehnia, Y. Rangraz and M. M. Heravi, *J. Organomet. Chem.*, 2021, **936**, 121712.
46. a) F. Monnier, F. Turtaut, L. Duroure and M. Taillefer, *Org. Lett.*, 2008, **10**, 3203-3206; b) C. Rajalakshmi, S. S. Jibin, R. Sulay, S. Asha, V. Ipe Thomas and G. Anilkumar, *Polyhedron*, 2021, **193**, 114869.
47. a) K. Okuro, M. Furuune, M. Enna, M. Miura and M. Nomura, *J. Org. Chem.*, 1993, **58**, 4716; b) L.-H. Zou, A. J. Johansson, E. Zuidema and C. Bolm, *Chem. Eur. J.*, 2013, **19**, 8144-8152.
48. M. B. Thathagar, J. Beckers and G. Rothenberg, *Green Chem.*, 2004, **6**, 215-218.
49. H. Oka, K. Kitai, T. Suzuki and Y. Obora, *RSC Adv.*, 2017, **7**, 22869-22874.
50. S. Kim, S. W. Kang, A. Kim, M. Yusuf, J. C. Park and K. H. Park, *RSC Adv.*, 2018, **8**, 6200-6205.
51. B. Wang, Y. Wang, X. Guo, Z. Jiao, G. Jin and X. Guo, *Catal. Commun.*, 2017, **101**, 36-39.
52. For selected reviews, see: a) N. Miyaura and A. Suzuki, *Chem. Rev.*, 1995, **95**, 2457; b) J. Hassan, M. Sevignon, C. Gozzi, E. Schulz and M. Lemaire, *Chem. Rev.*, 2002, **102**, 1359-1469; c) S. E. Hooshmand, B. Heidari, R. Sedghi and R. S. Varma, *Green Chem.*, 2019, **21**, 381-405.
53. Y. P. Budiman, A. Friedrich, U. Radius and T. B. Marder, *ChemCatChem*, 2019, **11**, 5387-5396.
54. M. B. Thathagar, J. Beckers and G. Rothenberg, *J. Am. Chem. Soc.*, 2002, **124**, 11858-11859.
55. a) K. Lamei, H. Eshghi, M. Bakavoli, S. A. Rounaghi and E. Esmaeili, *Catal. Commun.*, 2017, **92**, 40-45; b) S. Anuma and B. Ramachandra Bhat, *Mater. Today: Proc.*, 2019, **18**, 4942-4951.
56. G. Ranjani and R. Nagarajan, *Org. Lett.*, 2017, **19**, 3974-3977.
57. a) C. C. C. Johansson Seechurn, M. O. Kitching, T. J. Colacot and V. Snieckus, *Angew. Chem. Int. Ed.*, 2012, **51**, 5062-5085; b) K. C. Nicolaou, P. G. Bulger and D. Sarlah, *Angew. Chem., Int. Ed.*, 2005, **44**, 4442-4489.
58. For selected reviews, see: a) A. E. Shilov and G. B. Shul'pin, *Chem. Rev.*, 1997, **97**, 2879-2932; b) V. Ritleng, C. Sirlin and M. Pfeffer, *Chem. Rev.*, 2002, **102**, 1731-1769; c) D. Pla and M. Gomez, *ACS Catal.*, 2016, **6**, 3537-3552; d) T. Rogge, N. Kaplaneris, N. Chatani, J. Kim, S. Chang, B. Punji, L. L. Schafer, D. G. Musaev, J. Wencel-Delord, C. A. Roberts, R. Sarpong, Z. E. Wilson, M. A. Brimble, M. J. Johansson and L. Ackermann, *Nat. Rev. Methods Primers*, 2021, **1**, 43.

59. a) C. S. Yeung and V. M. Dong, *Chem. Rev.*, 2011, **111**, 1215-1292; b) I. Bosque, R. Chinchilla, J. C. Gonzalez-Gomez, D. Guijarro and F. Alonso, *Org. Chem. Front.*, 2020, **7**, 1717-1742; c) C.-J. Li, *Acc. Chem. Res.*, 2009, **42**, 335-344; d) K. Peng and Z.-B. Dong, *Adv. Synth. Catal.*, 2021, **363**, 1185-1201; e) A. M. F. Phillips, M. D. F. C. G. Da Silva and A. J. L. Pombeiro, *Catalysts*, 2020, **10**, 529.
60. a) C. M. A. Afsina, T. Aneeja, M. Neetha and G. Anilkumar, *Eur. J. Org. Chem.*, 2021, **2021**, 1776-1808; b) X. Zheng and Z. Li, in *From C-H to C-C Bonds: Cross-Dehydrogenative-Coupling*, ed. C.-J. Li, The Royal Society of Chemistry, 2015, pp. 55-66.
61. a) X. Marset, J. M. Perez and D. J. Ramon, *Green Chem.*, 2016, **18**, 826-833; b) S. Gupta, N. Chandna, P. Dubey, A. K. Singh and N. Jain, *Chem. Commun.*, 2018, **54**, 7511-7514; c) S. Gupta, H. Joshi, N. Jain and A. K. Singh, *J. Mol. Catal. A: Chem.*, 2016, **423**, 135-142.
62. For a revision concerning CDC mechanism under homogeneous regime, see: A. S. K. Tsang, S. J. Park and M. H. Todd, in *From C-H to C-C Bonds: Cross-Dehydrogenative-Coupling*, ed. C.-J. Li, The Royal Society of Chemistry, 2015, pp. 254-294.
63. F. Alonso, A. Arroyo, I. Martin-Garcia and Y. Moglie, *Adv. Synth. Catal.*, 2015, **357**, 3549-3561.
64. a) A. T. Nguyen, L. T. Pham, N. T. S. Phan and T. Truong, *Catal. Sci. Technol.*, 2014, **4**, 4281-4288; b) G. H. Dang, T. T. Dang, D. T. Le, T. Truong and N. T. S. Phan, *J. Catal.*, 2014, **319**, 258-264.
65. For selected reviews, see: a) Y. Volkova, S. Baranin and I. Zavarzin, *Adv. Synth. Catal.*, 2021, **363**, 40-61; b) B. V. Rokade, J. Barker and P. J. Guiry, *Chem. Soc. Rev.*, 2019, **48**, 4766-4790; c) V. A. Peshkov, O. P. Pereshivko and E. V. Van der Eycken, *Chem. Soc. Rev.*, 2012, **41**, 3790-3807.
66. M. Nasrollahzadeh, M. Sajjadi, F. Ghorbannezhad and S. M. Sajadi, *Chem. Rec.*, 2018, **18**, 1409-1473.
67. M. J. Albaladejo, F. Alonso, Y. Moglie and M. Yus, *Eur. J. Org. Chem.*, 2012, **2012**, 3093.
68. F. Ullmann, *Ber. Dtsch. Chem. Ges.*, 1903, **36**, 2382-2384.
69. C. Sambiagio, S. P. Marsden, A. J. Blacker and P. C. McGowan, *Chem. Soc. Rev.*, 2014, **43**, 3525-3550.
70. A. S. Guram, R. A. Rennels and S. L. Buchwald, *Angew. Chem. Int. Ed.*, 1995, **34**, 1348-1350.
71. J. F. Hartwig, S. Richards, D. Barañano and F. Paul, *J. Am. Chem. Soc.*, 1996, **118**, 3626-3633.
72. For a recent review, see: P. Ruiz-Castillo and S. L. Buchwald, *Chem. Rev.*, 2016, **116**, 12564-12649.
73. For selected reviews, see: a) J. Fairoosa, M. Neetha and G. Anilkumar, *RSC Adv.*, 2021, **11**, 3452-3469; b) N. K. Ojha, G. V. Zyryanov, A. Majee, V. N. Charushin, O. N. Chupakhin and S. Santra, *Coord. Chem. Rev.*, 2017, **353**, 1-57.
74. A. Srivastava and C. K. Jana, *Heterocycles via Cross Dehydrogenative Coupling*, Springer, 2019.
75. Q. Shuai, G. Deng, Z. Chua, D. S. Bohle and C.-J. Li, *Adv. Synth. Catal.*, 2010, **352**, 632-636.
76. M. Gopiraman and I. M. Chung, *J. Taiwan Inst. Chem. Eng.*, 2017, **81**, 455-464.
77. J. Zhang, C. Yu, S. Wang, C. Wan and Z. Wang, *Chem. Commun.*, 2010, **46**, 5244-5246.
78. T. Truong, G. H. Dang, N. V. Tran, N. T. Truong, D. T. Le and N. T. S. Phan, *J. Mol. Catal. A: Chem.*, 2015, **409**, 110-116.
79. S. Gupta, N. Chandna, A. K. Singh and N. Jain, *J. Org. Chem.*, 2018, **83**, 3226-3235.
80. For selected reviews, see: Q. Cai and W. Zhou, *Chin. J. Chem.*, 2020, **38**, 879-893.
81. B. Sreedhar, R. Arundhathi, P. L. Reddy and M. L. Kantam, *J. Org. Chem.*, 2009, **74**, 7951-7954.
82. H.-J. Xu, Y.-F. Liang, Z.-Y. Cai, H.-X. Qi, C.-Y. Yang and Y.-S. Feng, *J. Org. Chem.*, 2011, **76**, 2296-2300.
83. S. Ganesh Babu and R. Karvembu, *Ind. Eng. Chem. Res.*, 2011, **50**, 9594-9600.
84. M. Halder, M. M. Islam, Z. Ansari, S. Ahammed, K. Sen and S. M. Islam, *ACS Sustainable Chem. Eng.*, 2017, **5**, 648-657.
85. C. Galli and Z. Rappoport, *Acc. Chem. Res.*, 2003, **36**, 580-587.
86. A. R. Hajipour, F. Dordahan, F. Rafiee and M. Mahdavi, *Appl. Organomet. Chem.*, 2014, **28**, 809-813.
87. J. Lim, J. D. Kim, H. C. Choi and S. Lee, *J. Organomet. Chem.*, 2019, **902**.
88. A. R. Hajipour, M. Check and Z. Khorsandi, *Appl. Organomet. Chem.*, 2017, **31**, e3769.
89. S. R. Chaurasia and B. M. Bhanage, *Mol. Catal.*, 2020, **492**, 110998.
90. P. L. Reddy, R. Arundhathi and D. S. Rawat, *RSC Adv.*, 2015, **5**, 92121-92127.
91. A. Modi, W. Ali, P. R. Mohanta, N. Khatun and B. K. Patel, *ACS Sustain. Chem. Eng.*, 2015, **3**, 2582-2590.
92. D. M. T. Chan, K. L. Monaco, R.-P. Wang and M. P. Winters, *Tetrahedron Lett.*, 1998, **39**, 2933-2936.
93. P. Y. S. Lam, C. G. Clark, S. Saubern, J. Adams, M. P. Winters, D. M. T. Chan and A. Combs, *Tetrahedron Lett.*, 1998, **39**, 2941-2944.
94. For a recent review, see: J.-Q. Chen, J.-H. Li and Z.-B. Dong, *Adv. Synth. Catal.*, 2020, **362**, 3311-3331.
95. M. J. West, J. W. B. Fyfe, J. C. Vantourout and A. J. B. Watson, *Chem. Rev.*, 2019, **119**, 12491-12523.
96. a) S. K. Das, P. Deka, M. Chetia, R. C. Deka, P. Bharali and U. Bora, *Catal. Lett.*, 2018, **148**, 547-554; b) R. K. Borah, P. K. Raul, A. Mahanta, A. Shchukarev, J.-P. Mikkola and A. J. Thakur, *Synlett*, 2017, **28**, 1177-1182.
97. Y.-L. Cui, X.-N. Guo, Y.-Y. Wang and X.-Y. Guo, *Sci. Rep.*, 2015, **5**, 12005.
98. For selected reviews, see: a) M. Meldal and C. W. Tornoe, *Chem. Rev.*, 2008, **108**, 2952-3015; b) M. R. Decan, S. Impellizzeri, M. L. Marin and J. C. Scaiano, *Nat. Commun.*, 2014, **5**, 4612; c) N. Nebra and J. Garcia-Alvarez, *Molecules*, 2020, **25**, 2015; d) E. Haldon, M. C. Nicasio and P. J. Perez, *Org. Biomol. Chem.*, 2015, **13**, 9528-9550; e) C. Wang, D. Ikhlef, S. Kahlal, J.-Y. Saillard and D. Astruc, *Coord. Chem. Rev.*, 2016, **316**, 1-20; f) Y. Fang, K. Bao, P. Zhang, H. Sheng, Y. Yun, S.-X. Hu, D. Astruc and M. Zhu, *J. Am. Chem. Soc.*, 2021, **143**, 1768-1772.
99. R. Huisgen, *Angew. Chem. Int. Ed.*, 1963, **2**, 633-645.
100. C. W. Tornoe, C. Christensen and M. Meldal, *J. Org. Chem.*, 2002, **67**, 3057-3064.
101. V. V. Rostovtsev, L. G. Green, V. V. Fokin and K. B. Sharpless, *Angew. Chem., Int. Ed.*, 2002, **41**, 2596-2599.
102. For selected reviews, see: a) D. Dheer, V. Singh and R. Shankar, *Bioorg. Chem.*, 2017, **71**, 30-54; b) J. Huo, H. Hu, M. Zhang, X. Hu, M. Chen, D. Chen, J. Liu, G. Xiao, Y. Wang and Z. Wen, *RSC Adv.*, 2017, **7**, 2281-2287; c) A. Rani, G. Singh, A. Singh, U. Maqbool, G. Kaur and J. Singh, *RSC Adv.*, 2020, **10**, 5610-5635.
103. R. Hudson, C.-J. Li and A. Moores, *Green Chem.*, 2012, **14**, 622-624.

104. F. Chahdoura, C. Pradel and M. Gómez, *ChemCatChem*, 2014, **6**, 2929-2936.
105. M. Rodríguez-Rodríguez, P. Llanes, C. Pradel, M. A. Pericàs and M. Gómez, *Chem. Eur. J.*, 2016, **22**, 18247-18253.
106. F. Alonso, Y. Moglie, G. Radivoy and M. Yus, *J. Org. Chem.*, 2011, **76**, 8394-8405.
107. K. Chanda, S. Rej and M. H. Huang, *Chem. Eur. J.*, 2013, **19**, 16036-16043.
108. B. S. Lee, M. Yi, S. Y. Chu, J. Y. Lee, H. R. Kwon, K. R. Lee, D. Kang, W. S. Kim, H. B. Lim, J. Lee, H.-J. Youn, D. Y. Chi and N. H. Hur, *Chem. Commun.*, 2010, **46**, 3935-3937.
109. B. J. Borah, D. Dutta, P. P. Saikia, N. C. Barua and D. K. Dutta, *Green Chem.*, 2011, **13**, 3453-3460.
110. S. Mohammed, A. K. Padala, B. A. Dar, B. Singh, B. Sreedhar, R. A. Vishwakarma and S. B. Bharate, *Tetrahedron*, 2012, **68**, 8156-8162.
111. For a selected review, see: C. S. Demmer, N. Krogsgaard-Larsen and L. Bunch, *Chem. Rev.* , 2011, **111**, 7981-8006.
112. Y. Moglie, E. Mascaro, V. Gutierrez, F. Alonso and G. Radivoy, *J. Org. Chem.*, 2016, **81**, 1813-1818.
113. T. Yuan, F. Chen and G.-p. Lu, *New J. Chem.*, 2018, **42**, 13957-13962.
114. For selected reviews, see: a) C. J. Fui, M. S. Sarjadi, S. M. Sarkar and L. M. Rahman, *Catalysts*, 2020, **10**, 1103; b) H. Lin and D. Sun, *Org. Prep. Proced. Int.*, 2013, **45**, 341-394.
115. D. Das, *ChemistrySelect*, 2016, **1**, 1959-1980.
116. K. Mullick, S. Biswas, C. Kim, R. Ramprasad, A. M. Angeles-Boza and S. L. Suib, *Inorg. Chem.*, 2017, **56**, 10290-10297.
117. M. Trivedi, S. k. Ujjain, R. K. Sharma, G. Singh, A. Kumar and N. P. Rath, *New J. Chem.*, 2014, **38**, 4267-4274.
118. S. G. Babu and R. Karvembu, *Tetrahedron Lett.*, 2013, **54**, 1677-1680.
119. Z. Zhai, X. Guo, Z. Jiao, G. Jin and X.-Y. Guo, *Catal. Sci. Technol.*, 2014, **4**, 4196-4199.
120. F. Niu, Y. Jiang and W. Song, *Nano Res.*, 2010, **3**, 757-763.
121. M. Puri, S. Gatard, D. A. Smith and O. V. Ozerov, *Organometallics*, 2011, **30**, 2472-2482.
122. T. T. Tsou and J. K. Kochi, *J. Am. Chem. Soc.*, 1979, **101**, 6319.
123. C. Amatore, M. Azzabi and A. Jutand, *J. Am. Chem. Soc.*, 1991, **113**, 8375.
124. a) A. Casitas, A. E. King, T. Parella, M. Costas, S. S. Stahl and X. Ribas, *Chem. Sci.*, 2010, **1**, 326-330; b) F. Monnier and M. Taillefer, *Angew. Chem., Int. Ed.*, 2009, **48**, 6954-6971.
125. Y. Isomura, T. Narushima, H. Kawasaki, T. Yonezawa and Y. Obora, *Chem. Commun.* , 2012, **48**, 3784-3786.
126. A. S. Singh, S. S. Shendage and J. M. Nagarkar, *Tetrahedron Lett.*, 2014, **55**, 4917-4922.
127. S. A. Mousavi Mashhadi, M. Z. Kassaee and E. Eidi, *Appl. Organomet. Chem.*, 2019, **33**, e5042.
128. R. K. Sharma, R. Gaur, M. Yadav, A. K. Rathi, J. Pechousek, M. Petr, R. Zboril and M. B. Gawande, *ChemCatChem*, 2015, **7**, 3495-3502.
129. C. Gonzalez-Arellano, R. Luque and D. J. Macquarrie, *Chem. Commun.*, 2009, DOI: 10.1039/b818767c, 1410-1412.
130. P. Zhang, J. Yuan, H. Li, X. Liu, X. Xu, M. Antonietti and Y. Wang, *RSC Adv.*, 2013, **3**, 1890-1895.
131. K. H. V. Reddy, V. P. Reddy, J. Shankar, B. Madhav, B. S. P. Anil Kumar and Y. V. D. Nageswar, *Tetrahedron Lett.*, 2011, **52**, 2679-2682.
132. V. K. Akkilagunta and R. R. Kakulapati, *J. Org. Chem.*, 2011, **76**, 6819-6824.
133. S. Wang, Y. Yu, J. Yu, T. Wang, P. Wang, Y. Li, X. Zhang, L. Zhang, Z. Hu, J. Chen, Y. Fu and W. Qi, *Nanotechnology*, 2020, **31**, 255604.
134. V. P. Reddy, A. V. Kumar and K. R. Rao, *J. Org. Chem.*, 2010, **75**, 8720-8723.
135. M. Soleiman-Beigi, I. Yavari and F. Sadeghizadeh, *Chem. Pap.*, 2018, **72**, 2239-2246.
136. V. P. Reddy, A. V. Kumar, K. Swapna and K. R. Rao, *Org. Lett.*, 2009, **11**, 951-953.

